

Immobilized Photosensitisers for antimicrobial applications

Cinzia Spagnul,^a Lauren C. Turner,^a Ross W. Boyle ^{*a}

^a Department of Chemistry, University of Hull, Kingston-upon-Hull, East

Yorkshire, HU6 7RX, UK

* corresponding author: E-mail: r.w.boyle@hull.ac.uk, Telephone: +44 (0)1482 466353, Fax: +44 (0)1482 466410

Abstract

Photodynamic antimicrobial chemotherapy (PACT) is a very promising alternative to conventional antibiotics for the efficient inactivation of pathogenic microorganisms; this is due to the fact that it is virtually impossible for resistant strains to develop due to the mode of action employed. PACT employs a photosensitizer, which preferentially associates with the microorganism, and is then activated with non-thermal visible light of appropriate wavelength(s) to generate high localized concentrations of reactive oxygen species (ROS), inactivating the microorganism.

The concept of using photosensitizers immobilized on a surface for this purpose is intended to address a range of economic, ecological and public health issues.

Photosensitising molecules that have been immobilized on solid support for PACT applications are described herein. Different supports have been analyzed as well as the target microorganism and the effectiveness of particular combinations of support and photosensitiser.

Keywords: Photodynamic antimicrobial chemotherapy, Pathogen inactivation, Photosensitizer immobilized, disinfection, Reactive Oxygen Species

Contents:

1. Introduction.....	3
2. Phenothiazinium based photobactericidal materials.....	7
3. Ruthenium complexes	12
4. Rose Bengal	14
5. Phthalocyanines	18
6. Porphyrins immobilized on Natural Polymers	21
7. Porphyrins linked to synthetic polymers	24
8. Others Photosensitiers	32
9. Conclusions.....	33

31	10.	Appendix: Table and Abbreviations	34
32	11.	References	40
33			

34 1. Introduction

35 Nosocomial infections or “Healthcare Associated Infections” (HAI) can cause disability and
36 emotional stress for the patient and may, in some cases, lead to disabling conditions or even death.
37 In addition, since infected patients remain in hospital on average 2.5 times longer than uninfected
38 patients the economic cost derived by the increased length of stay for infected patients is
39 considerable [1,2]. In Europe every year healthcare associated infections cause 25 million extra-
40 days of hospital stay, 37,000 attributable deaths, and contribute to an additional 135,000 deaths
41 every year with a corresponding economic burden of €13–24 billion [3], while in the United States
42 it is estimated that about two million patients develop HAI with a total number of deaths of 99,000,
43 and cost of \$33 billion each year [1].

44 The Centre for Disease Control and Prevention has recognized that contaminated environmental
45 surfaces provide an important potential source for indirect transmission of many healthcare-
46 associated pathogens and contribute to the spreading of infections, thus indicating the need for new
47 and sustainable strategies [4,5,6,7].

48 Another major challenge is associated with the large number of water-borne diseases which arise
49 from contaminated water [8].

50 Worldwide 884 million people lack access to clean potable water: developing countries lack access
51 to clean water (1.8 million children die every year from diarrhea) [9], while developed countries
52 face an urgent need to provide efficient waste water treatment, as populations grow. The increasing
53 prevalence of bacterial resistance is another problem for which an urgent solution is needed.

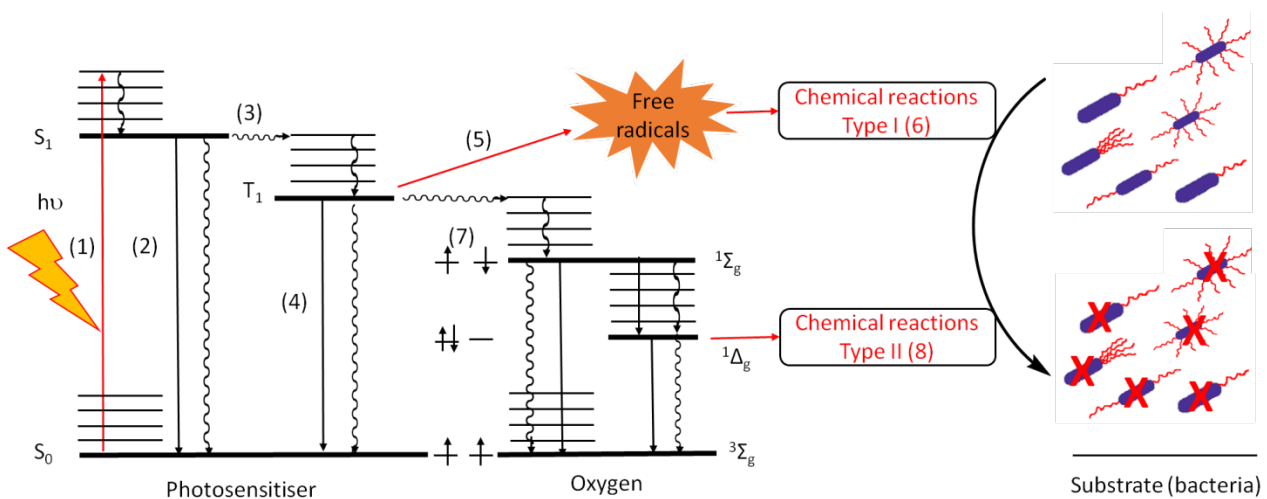
54 In fact, the traditional methods for water disinfection currently used are effective against bacteria
55 and viruses but have their drawbacks: chlorine disinfection can produce carcinogenic by-products
56 when organic compounds are present in the water [10], whilst use of ozone is expensive and
57 requires *in situ* generation due to its unstable nature [11,12,13]. Thermal [14] and UV-based [15]
58 disinfections require excessive amounts of energy, and thus are expensive and non eco-friendly.

59 Photodynamic antimicrobial chemotherapy (PACT) offers an alternative, and radically different,
60 strategy for the inactivation of pathogenic micro-organisms [16,17,18,19]

61 PACT is based on the “photodynamic effect” where a photosensitizer, preferentially associated with
62 a microorganism, is activated with non-thermal visible light of appropriate wavelength(s) to
63 generate toxic species that inactivate the microorganism.

64 Upon absorption of a photon, the photosensitizer (Ps) is promoted from a lower-energy ‘ground
65 state’ to a higher-energy singlet state (S) and then, by intersystem crossing, it can convert to an

66 excited triplet state (T). From the, relatively, long lived triplet state it can then follow two
 67 photochemical pathways, named Type I and Type II reactions (Fig. 1).
 68 In the Type I mechanism, Ps molecules react with bio-organic molecules such as the cell membrane
 69 constituents and transfer a proton or an electron to form free radicals and radical ions. In a Type II
 70 reaction, the excited Ps can transfer its energy directly to molecular oxygen resulting in production
 71 of reactive oxygen species (ROS) that are able to kill microbial cells and viruses [20,21].
 72 Finally, the ability to inactivate microorganisms without inducing resistance makes PACT an
 73 appealing and useful alternative in treating infections [22,23].



74
 75 **Fig. 1:** Jablonski diagram showing the various modes of excitation and relaxation in a
 76 chromophore. Light of an appropriate wavelength is absorbed by the photosensitizer molecule.
 77 Thereby the photosensitizer changes from its initial ground state (S_0) into an energetically excited
 78 state (S_1). From this state the molecule can return to its ground state through (2) = fluorescence
 79 emission (3) = intersystem crossing.
 80 Provided that the triplet T_1 state is long-lived in comparison to S_1 , it can return to its ground state
 81 by (4) = phosphorescence emission or it can (5) = react with surrounding molecules to produce (6)
 82 = Type I reactions with free radicals. Otherwise it can react with oxygen to produce (7) = spin
 83 exchange and (8) = Type II reactions (1O_2). Singlet oxygen is highly reactive and plays a major role
 84 in photodynamic inactivation of pathogens. Curved arrows describe internal conversion and in
 85 general loss of energy.

86 In most cases, Gram (+) and Gram (-) bacteria are susceptible to the photosensitizing action of a
 87 variety of sensitizers under appropriate conditions. Examples of photodynamic inactivation of
 88 various Gram (+) and Gram (-) bacteria [24], such as *E. coli* [25,26], *S. aureus* [26,27], *S. mutans*
 89 [28], *P. gingivalis* [29], and *P. aeruginosa* [27,30] have been documented in the literature.
 90 Various studies have shown that there is a fundamental difference in susceptibility to PACT
 91 between Gram (+) and Gram (-) bacteria.

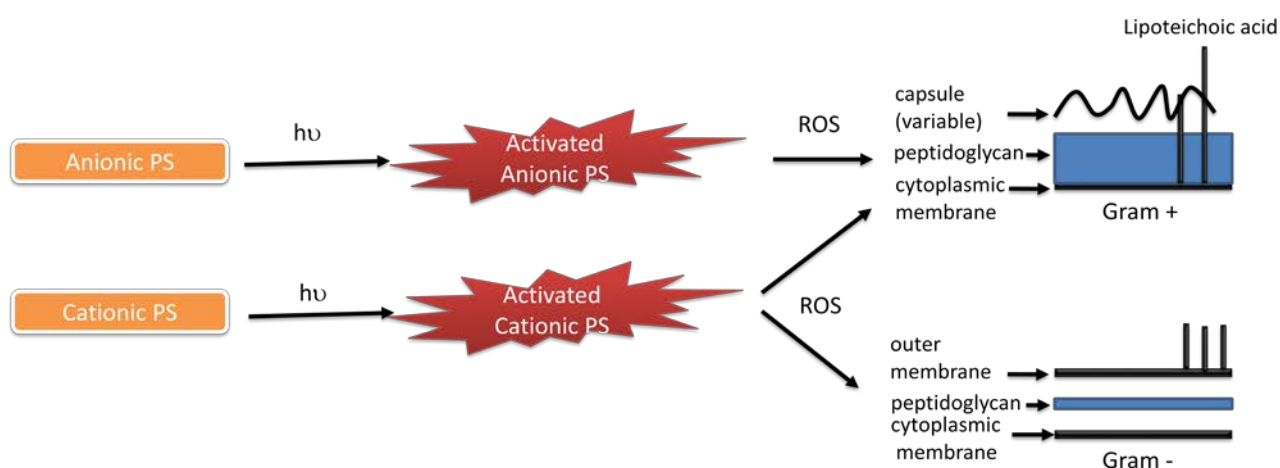
92 Gram (+) species are more susceptible towards PACT inactivation because their outer wall, located
93 outside the cytoplasmic membrane, is a relatively porous structure that is permeable to nutrients,
94 glycopeptides and polysaccharides with a molecular weight in the 30,000–60,000 Da range and in
95 the same way it allows photosensitisers to cross [31].

96 Gram (–) bacteria are characterized by the presence of an additional 10-15 nm thick and highly
97 organized outer membrane, which inhibits the penetration of some photosensitisers and
98 photogenerated reactive species [32].

99 Only relatively hydrophilic compounds with a molecular weight lower than 600–700Da can diffuse
100 through the porin channels that are located in the outer membrane [33].

101 Since the Gram (–) outer membrane is more negatively charged [34], cationic hydrophilic
102 photosensitizers are attracted to it, while anionic photosensitizers are repelled, and thus are
103 generally only active against Gram (+) bacteria (Fig. 2).

104 Cationic photosensitizers or anionic photosensitizers co-administrated with an outer membrane
105 disrupting agent can, however, inactivate both Gram (+) and Gram (–) microorganisms.



106

107 **Fig. 2.** Schematic representation of antimicrobial PDT. The photosensitizer (Ps) in the presence of
108 light becomes excited and produces toxic oxygen species which damage DNA and/or membrane
109 sites. Anionic photosensitizers are generally active only against Gram (+) bacteria because they
110 cannot permeate the more negatively charged Gram (–) outer membrane [35].

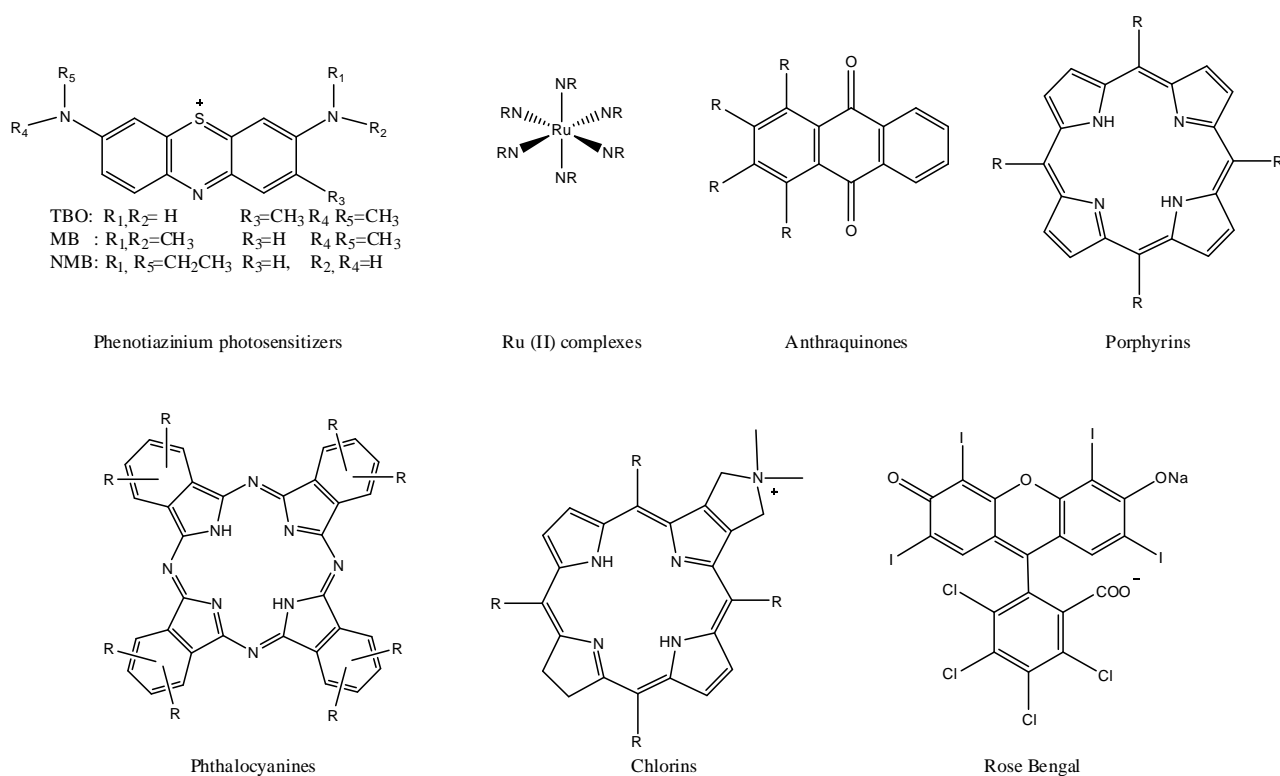
111 A wide variety of cationic and anionic photosensitizers, such as Rose Bengal (RB), porphyrins,
112 phthalocyanines (Pc), methylene blue (MB), toluidine blue O (TBO), anthraquinones and ruthenium
113 complexes have been utilised for PACT in solution/suspension [36,37,38,39,40].

114 Ideally, since the Ps do not have to penetrate the bacterium or even come into a contact with the
115 cell in order to be effective [41], immobilization of the photosensitiser aims to allow both the

116 efficient elimination of microorganisms, possibly during several cycles of use, and also the
117 complete photosensitiser removal from the treated medium.

118 Other possible benefits include, reuse of the Ps and the possibility of water recycling after
119 disinfection, and the gradual photobleaching of the dyes by solar light, which prevents their
120 accumulation in the environment.

121 Many patents [42] and publications describe the immobilization of photosensitisers to combat
122 bacterial infections. The aim of this review is to present the photosensitising molecules that have
123 been immobilized on a support, the different supports utilized, and the bacteria that can be
124 inactivated using particular combinations of support and photosensitiser (Table 1) (Fig 3).



126 **Fig 3.** Natural and synthetic photosensitizing unit described in this review used in PACT.

2. Phenothiazinium based photobactericidal materials

Methylene Blue (MB) and Toluidine Blue O (TBO) have great potential applications in PACT due to their low toxicity, the presence of a positive charge that makes them active against both Gram (+) and Gram (–) bacteria, and their favorable photochemical and photophysical characteristics such as light absorption at 650 nm. Both of these photosensitising molecules can be used as PACT agents [43,44,45] for inactivation of viruses and bacteria in blood fractions, and for plasma sterilization [46].

MB and TBO have been incorporated into silicone [47,48,49,50], polyurethane [51,52], polyethylene [53], cellulose acetate [54,55,56], plastics commonly used to fabricate devices used in hospitals such as catheters, and the photoantimicrobial ability of the resulting materials evaluated.

Cahan et al. [53] developed an inexpensive and simple method for preparing antibacterial surfaces by spreading a mixed powder of poly (vinylidene fluoride) nanobeads and three photosensitizers (RB, MB or TBO, 1:10 wt/wt each and previously immobilized on the same type of nanobeads) on the surface of a thermoplastic, low-density polyethylene film (thickness 100 μm). The sandwich layers were covered with a crimped stamp and exposed to a hot pressing device for 1 h at 95° C. The polyethylene layer was softened under the heat pressing and it trapped the nanobeads with and without the Ps, which remained solid under the pressing temperature. Goniometrical measurements confirmed the hydrophobicity of all the surfaces and energy dispersive X-ray spectroscopy (EDS) analysis was used to determine the concentration of the photosensitisers on the surface, that were 4.59 % and 1.68 % wt/wt, respectively for the MB and TBO, while the concentration of RB on the surface was undetectable, probably because it was below the 1 %, detection limit for this mode of analysis. Significant reactive oxygen species were generated after illumination of the immobilized photosensitizers with a light fluence rate of 1.46 mW cm^{-2} for 30 minutes. Photodynamic inactivation assays performed in nutrient broths under similar conditions for 24 h demonstrated an increase in the antibacterial activity of the photoactive materials as a function of the initial bacterial cell concentration (10^3 , 10^5 and 10^7 CFU mL^{-1} for *E. coli*) increasing to more than 4 \log_{10} reduction of the attached *E. coli* after illumination (1.46 mW cm^{-2}) for 24 h when the inoculum was 10^3 CFU mL^{-1} . However, with the same inoculum, more than 4 log reduction of *S. aureus* was observed when the cultures were illuminated for 6 h, showing that Gram (+) cells are significantly more sensitive to the antibacterial effect of the surfaces than Gram (–).

Dyes were also incorporated together with nanogold into medical grade polymers commonly used in urinary catheter devices i.e. silicone and polyurethane using the “swell-encapsulation-shrink” method. An appropriate mixed solvent system allowed the polymer to swell thus enabling both dye and the nanoparticles (if used) to enter into the polymer matrix. After drying in air to allow

161 evaporation of the solvent mixture, the polymer contracted to its original size, resulting in strongly
162 colored dye-encapsulated polymer [48,49,50,51,52,57]. These antimicrobial polymers show
163 significant antimicrobial activity against *S. aureus* and *S. aureus* (MRSA) when exposed to white
164 light for 24 hours [50,51] or for 1 to 10 min against *S. aureus* (MRSA), *E. coli*, *S. epidermidis* when
165 exposed to light from a low power 660 nm laser [48,49,52,57].

166 Interestingly, the material properties, with regard to both the surface roughness and elasticity were
167 investigated before and after the exposure to radical species [47]. It is known that the radical species
168 produced during gas plasma sterilization result in a decrease of elasticity of the polyurethane and an
169 increase in brittleness, both undesired effects as they would cause problems during catheter removal
170 [58,59].

171 The result demonstrated that exposure to laser light did not modify the elasticity (Young's
172 modulus), the friction coefficient [52] or breaking point of the silicone containing photosensitizer.
173 The surface roughness of the material and other surface topography parameters, such as the asperity
174 density and the asperity height showed instead a continuous decrease with energy dose, thus making
175 the material less prone to microbial adhesion [47]. The authors also demonstrated that a laser
176 irradiation performed for 10 mins every 60 mins for 6 hours can inhibit biofilm formation and can
177 reduce the extent of surface colonization.

178 Furthermore, since the irradiated material didn't become more brittle, this makes the light-activated
179 material still suitable for catheter production since a reduction in elasticity would make the material
180 more brittle causing problems during catheter insertion/removal [47].

181 TBO was incorporated into cellulose acetate polymer, which could be applied as a coating (either
182 permanently or on a renewable basis) to hospital surfaces for surface disinfection [54,55,56]. The
183 ability of TBO to kill a range of microbes under lighting conditions similar to those present in
184 hospitals was evaluated.

185 The incorporation of TBO into cellulose acetate resulted in an antimicrobial material that can kill
186 effectively both a methicillin-resistant strain of *S. aureus* (EMRSA) and *P. aeruginosa* in 24 hours
187 eradicating in the order of 10^5 CFU/cm² of both bacteria over a 24 hour period using white light
188 illumination (60 W domestic lamp bulb), a level adequate to potentially reduce the bacterial
189 population found on common surfaces in hospitals [54].

190 The antimicrobial TBO cellulose acetate polymer demonstrated a potent photoinactivation of a
191 range of microorganisms such as *S. aureus*, *E. coli*, *C. albicans*, *C. difficile*, and bacteriophage
192 X174 (host organism, *E. coli* ATCC 13706) upon illumination with a white light source (28 W
193 fluorescent lamp) for periods ranging from 2 h to 16 h [55]. *C. albicans* was found to be the least

194 sensitive to photosensitization using this system, with an 88% reduction in the viable count of *C.*
195 *albicans* after 16 h irradiation. [55]

196 Furthermore, Decraene evaluated the effectiveness of the coatings against microbes deposited onto
197 surface from aerosols, as this is closer to the true situation found in hospitals [56].

198 Interesting, for *E. coli* the efficacy of bacterial photoinactivation was found to be dependent on the
199 fluid the bacteria was suspended in with greater values for PBS than for human saliva, or horse
200 serum (99.8 %, 97.6 % and 78.9 % respectively).

201 TBO was also conjugated to chitosan and this resulted in an improved efficacy against biofilm cells
202 of *S. aureus* (MRSA) and planktonic cells of *P. aeruginosa*, and *A. baumannii*. Chitosan alone and
203 without illumination had no antimicrobial activity, suggesting that the potentiated effect of chitosan
204 worked after the bacterial damage induced by PACT [60].

205 TBO was also incorporated into a mucoadhesive patch as a potential delivery system for use in
206 PACT of oropharyngeal candidiasis [61].

207 The authors also investigated the effect on *C. albicans* biofilms using TBO and illumination at 635
208 nm. With biofilms, higher concentrations of TBO and longer incubation times were required to
209 achieve a total inactivation of biofilms than for planktonic cells. Therefore, the authors suggested
210 that short application times of TBO-containing mucoadhesive patches should allow treatment of
211 recently acquired oropharyngeal candidiasis, whereas longer times are required for persistent
212 disease where biofilms are already formed [61].

213 Wainwright et al. [62] dispersed new methylene blue, a methylene blue analogue, in urethane-
214 acrylate and styrene-butadiene copolymers (40% w/w) and the antimicrobial activity of the resultant
215 copolymer films was tested against both *S. epidermis* and *E. coli* bacteria.

216 When compared to polyacrylic ester films, the MB-containing styrene-butadiene films exhibited a
217 greater antibacterial activity. This might be related to the different hydrophobicities of the two
218 polymer types. Overall, the antimicrobial activity was more evident against the Gram (+) bacteria *S.*
219 *epidermidis*, than the Gram (-) bacteria *E. coli*. Furthermore, for both bacterial strains,
220 photodynamic inactivation assays gave the best results at both highest photosensitizer concentration
221 (1000 μM) and highest light dose (11.5 J cm^{-2}).

222 Piccirillo et al. [49] reported the first example of TBO covalently bound at the surface of an
223 activated silicone polymer. The antibacterial efficiency was tested against *E. coli* and *S. epidermidis*
224 by exposure to 634 nm laser light. The polymer possessed significant activity even when the dye
225 was present at a relatively low concentration, probably because the dye was held at the surface and
226 the generated ROS were in the best position to interact with bacteria, owing to their short diffusion
227 distances.

228 It was found that the presence of 2 nm in diameter gold nanoparticles synergistically enhanced the
229 killing of *E. coli* and *S. epidermidis* when encapsulated in silicone with MB even though the
230 mechanism of action is still poorly understood [48].

231 In another study, a polysiloxane polymer embedded with MB and 2 nm nanogold particles showed
232 up to a 3.5 log₁₀ reduction of *S. aureus* (MRSA) and *E. coli* when exposed for 5 min to a low power
233 600 nm laser. [57]

234 Naik et al. [51] incorporated MB and TBO with gold nanoparticles into polyurethane. When
235 irradiated with white light for 24 hours, MB and TBO impregnated polyurethane polymers showed
236 a 2.8 log and 4.3 log reduction in *S. aureus* respectively. An additional 1 log₁₀ reduction in bacteria
237 in the case of MB and 0.5 log in the case of TBO was observed when the gold nanoparticles were
238 incorporated with the two photosensitizers.

239 Interestingly, in both cases the incorporation of 2 nm nanogold particles significantly enhanced the
240 ability of MB to kill bacteria even though the mechanism of action is still poorly understood. It has
241 been hypothesized that the gold nanoparticles might enhance the hydrophobic properties of the
242 polymer or they might increase the kinetics of the reactions between the ROS generated by the
243 photosensitizers and the microorganisms.

244 Since it is known that optical and electronic properties of gold nanoparticles are affected by their
245 size, Perni et al [48] studied the effect of the size of the gold nanoparticles on the antimicrobial
246 properties of MB silicone polymer demonstrating an enhanced light-activated antimicrobial activity
247 against Gram (+) and Gram (-) bacteria for nanoparticles of 2 nm.

248 Another study by Perni [52] however, indicated that the presence of nanogold did not improve the
249 antimicrobial activity of TBO embedded in polyurethane, even if the uptake of TBO in
250 polyurethane was higher than that reported for silicone. This might be due to the inaccessibility of
251 the dye entrapped in the polyurethane. In fact, a study of suspended TBO-tiopronin-gold
252 nanoparticle in aqueous solution demonstrated a four-fold decrease in minimum bactericidal
253 concentration under white light or 632 nm laser illumination when compared with the free TBO.
254 [63].

255 In an earlier paper, Savino [64] reported a MB conjugate, where the photosensitizer was covalently
256 immobilized on 2% poly(styrene) copolymer by nitration, reduction and diazotization. That
257 conjugate was found able to disinfect contaminated tap water with *E. coli* to levels acceptable for
258 drinking.

259 MB and TBO are active against a wide range of bacteria and viruses and they have been
260 successfully immobilized in a wide range of polymers, showing the ability to inactivate bacteria and
261 viruses even under light conditions similar to those commonly used in hospitals. Those materials in

262 the future may play an important role in decreasing the incidence and the spreading of nosocomial
263 infection. They can find other key applications, such as the development of devices to disinfect
264 water.

265 The field still faces with the key challenge of having a photobactericidal material with significant
266 activity and with the dye present at as the lowest concentration as possible, avoiding the leaching of
267 the dye from the material, a problem that has been observed sometimes. A covalent attachment of
268 the phenothiazinum dyes to the surface of the inert support may minimize the leaching of the
269 biocidal agent into the surrounding environment and prevent aggregation.

270 3. Ruthenium complexes

271 Ru(II) metal complexes with ligands, such as 2, 2'-bipyridine (bpy) [65,66] and 1,10-
272 phenanthroline-5,6-dione (phendione) [67] recently showed remarkable photo-killing ability and
273 therefore potential PACT applications. In fact those compounds appear particularly appealing due
274 to the intrinsic positive charges and the consequent potent binding capacity to the negatively
275 charged outer membrane of Gram (-) bacteria i.e. *E. coli* [68], the production of ROS [69,70], and
276 the possibility of assembling peripheral ligands around the central metal to design a transition-metal
277 complex with favorable functions such as, water solubility and biological compatibility.

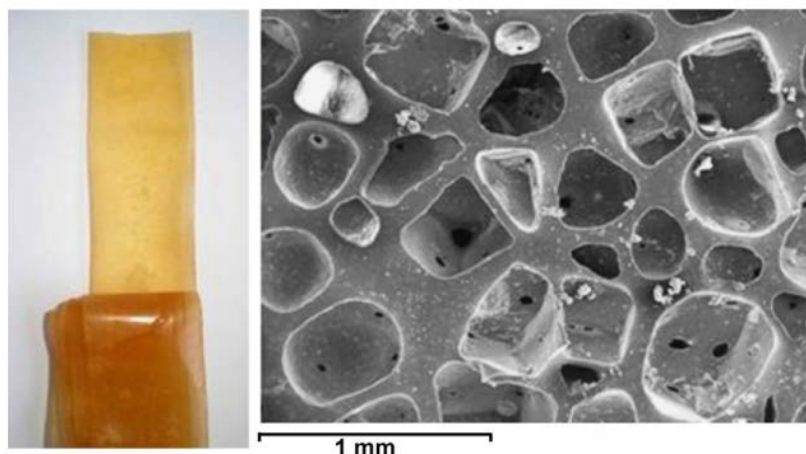
278 Bourdelande et al. [71] demonstrated that aqueous suspensions of a Ru(II) complex, $[\text{Ru}(\text{bpac})_3]^{2+}$
279 where bpac = 4,4'-dicarboxy-2,2'-bipyridine, both free in solution and covalently immobilized on
280 Sephadex G-25 (a hydrophilic resin formed by copolymerization of dextran and epichlorohydrine)
281 forming an insoluble hydrophilic polymer, are able to effectively generate singlet oxygen.

282 With the aim of carrying out a laboratory-to-pilot-installation study on water disinfection by
283 polymer-supported Ru(II) complexes, porous silicone hollow cylinders, cationic derivatives of
284 nylon, poly(vinylidene difluoride) (PVDF) membranes and cellulose membranes were selected to
285 immobilized different Ru(II) complexes, such as [tris(4,7-diphenyl-1,10-phenanthroline)-
286 ruthenium(II)] dichloride, tris(1,10-phenanthrolinyl-4,7-bis(benzenesulfonate) ruthenate(II)) and
287 tris(4,4'-dinonyl-1,10 phenanthroline)ruthenium(II) from concentrated hydroalcoholic or aqueous
288 solutions (typically in the mM range) until saturation of the support was achieved [72].

289 Among all the different couples investigated, [tris(4,7-diphenyl-1,10-phenanthroline)-
290 ruthenium(II)] dichloride (abbreviated RDP²⁺) embedded in porous silicone hollow cylinders
291 yielded the best combination of O₂ quenching efficiency and singlet oxygen lifetime, efficient
292 singlet oxygen generation and bactericidal action against *E. coli* and *E. faecalis* under sunlight with
293 no photosensitizer leaching into the water.

294 On the contrary, significant leaching was observed with tris(1,10-phenanthrolinyl-4,7-
295 bis(benzenesulfonate) ruthenate(II)) embedded in cationic nylon and cellulose membrane.

296 Manjon [73,74,75] and Villien [76] (Fig. 4.) recently evaluated the efficiency of different ¹O₂
297 photosensitizing Ru(II) tris-chelate complexes immobilized on anionic and cationic porous silicone
298 in solar reactor prototypes for the disinfection of water contaminated with *E. coli* or *E. faecalis*.
299 Anionic and cationic porous silicone were selected as support due to their optical transparency in
300 the visible region, excellent oxygen permeability, the durability and the porosity, that increases the
301 accessibility of the lethal ROS to the target microorganisms (Fig. 4).



302

303 **Fig. 4.** Photograph of a 35 mm wide porous silicone (pSil) stripe with RDP²⁺ photosensitizer dye
304 (left) and a scanning electron micrograph of an undyed porous silicone strip (right) [76].

305

306 All provided significant inactivation using both artificial light or exposing the silicone strips to
307 sunlight. Furthermore, the solid support proved to be reusable after reloading the sunlight-bleached
308 substrate with new photosensitising material [75].

309 The recovery and reuse of immobilized photosensitizer opens the possibility to apply the
310 photodynamic process in a real waste treatment system, avoiding the photosensitizer release and
311 consequent contamination of water effluents.

312 Manjon et al. [73] synthesized a new photosensitising material where C₆₀-fullerene and tris(4,7-
313 diphenyl-1,10-phenanthroline)ruthenium(II) dichloride were embedded into porous silicone using
314 the swell-encapsulation-shrink method. That material had favorable photophysical properties, but
315 exhibited poor inactivation of waterborne bacteria due to aggregation.

316 Ru(II) based photokilling materials only recently have showed photobactericidal properties, thus
317 offering the possibility of new developments for PACT applications. The possibility to turn the
318 properties of the desired complex by changing the peripheral ligands is a key property that can be
319 used to develop highly efficient photosensitizers to combat antibiotic resistant pathogenic bacteria
320 and to create new photobactericidal materials that may have potential key applications in domestic
321 and healthcare settings.

322 4. Rose Bengal

323 Rose Bengal (RB) is a commercially available, highly water soluble anionic photosensitizer with
324 high singlet oxygen quantum yield, low rate of photodegradation and with a remarkable
325 antibacterial activity against Gram (+) bacteria [77] when irradiated with simulated sunlight [78].

326 The cellular envelope has been identified as a probable target [79].

327 To increase the killing efficiency against both Gram (+) and Gram (-) bacteria at lower
328 concentrations, RB has been incorporated into natural polymers, such as cellulose acetate [55,56]
329 and chitosan [80,81,82,83,84,85].

330 Chitosan (CS), the N-deacetylated derivative of chitin, is a natural linear biopolyaminosaccharide
331 consisting of 1,4-linked N-acetyl-D-glucosamine (GlcNAc) and D-glucosamine (GlcN).

332 It is inexpensive, biodegradable, and nontoxic for mammals. It has an antimicrobial activity itself
333 [86,87] and it possess free amino groups, which makes it attractive for the development of new
334 chemical bonds. Due to these favorable characteristics, it has received significant interest in a broad
335 range of scientific areas such as the food industry [88], cosmetics [89], pharmaceutical and
336 biomedical sciences [90] such as dentistry [91].

337 Moczek et al. proved that RB attached to the chitosan did not decrease the photosensitizing activity
338 of the chromophore when attached through dehydration or covalent linkage to form two conjugates
339 with different degrees of substitution with RB [80].

340 The content of RB attached to the polymer was found to be 0.013 mol % for the conjugate obtained
341 through dehydration and 0.35 mol % for the conjugate obtained through covalent linkage with
342 respect to the glucosamine unit of the chitosan, respectively.

343 Results indicated that the shape of the absorption spectrum and the ratio of the absorbance at the
344 maxima were not dependent on polymer concentration in the range studied (1–0.1 g/L), and the
345 quantum yield of singlet oxygen formed by RB after conjugation with chitosan was very similar to
346 free RB in water.

347 Since chitosan has mucoadhesive properties, the possibility to use CS nanoparticles functionalized
348 with photosensitizer RB (CSRBnp) was explored in dentistry to improve root canal disinfection
349 [85] even in the presence of tissue inhibitors within root canals [82].

350 *E. faecalis*, a Gram (+) facultative microbe, was selected as a model since it plays an important role
351 in the biofilm formation on biomedical devices and it is frequently the only surviving bacterium in
352 recurrent root canal infection.

353 Chitosan nanoparticles were functionalized with RB to provide a single-step treatment in a
354 synergistic approach combining the antibacterial properties of the conjugate and the chitosan
355 reinforcing ability on dentin-matrix [81].

356 RB was immobilized onto chitosan nanoparticles *via* amide bonds using N-ethyl-N'-(3-dimethyl
357 aminopropyl) carbodiimide (EDC) and N-hydroxysuccinimide (NHS) as coupling agents.

358 Based on the absorption spectra, the amount of RB bound in the conjugated CSRBnp was
359 calculated to be 14 μ M per 0.1 mg/mL. Photocytotoxicity studies revealed higher fibroblast cell
360 survival, where compared to RB alone highlighting the biocompatibility of the conjugate [81].

361 When tested on planktonic cultures and biofilms of *E. faecalis*, a similar CSRBnp conjugate, but
362 with a lower concentration of RB bound in the conjugate (3 μ M in 0.3 mg/ml of CSRB),
363 demonstrated better PACT efficacy than RB alone [85].

364 When dentin collagen was crosslinked to CSRBnp, the CSRBnp-cross-linked dentin collagen
365 showed higher resistance to collagenase degradation and superior mechanical properties [81].

366 The antibacterial and antibiofilm efficacy of a polycationic chitosan-conjugated Rose Bengal
367 photosensitizer (CSRB) were also tested on *P. aeruginosa* (Gram $-$) [84] since *Pseudomonas*
368 species are frequently associated with chronic infections and they have been detected in persistent
369 root canal infections. Concentration of CSRB uptaken by the bacterial biofilms was significantly
370 higher than that of RB alone, especially in the biofilms. Photoactivation studies resulted in
371 significantly higher elimination of bacterial biofilms with CSRB than RB alone, highlighting the
372 advantage of using polycationic CSRB over anionic RB to achieve improved antibiofilm efficacy.

373 Rose Bengal and chitosan were covalently attached to the surface of polydimethylsiloxane (PDMS)
374 through a two-step argon plasma treatment. First acrylic acid was grafted onto PDMS to form
375 PDMS-pAAc films that were further conjugated to CH.RB through chitosan amino groups, via
376 EDC/NHS mediated coupling [83]. The amount of RB present in the CH.RB conjugate was found
377 to be 0.1 mol% by UV-vis spectroscopy at 575 nm and the grafted CH.RB was estimated to be 10.4
378 ± 0.1 mg/cm² on PDMS-pAAc films.

379 Preliminary antibacterial testing against *S. aureus* and *E. coli* revealed that the system might be
380 potentially applicable towards Gram (+) bacteria.

381 Decraene et al. [55] investigated the photokilling ability of RB immobilized together with TBO at
382 the same concentrations on cellulose acetate by evaporation of acetone. They showed that the
383 leakage of photosensitizer was extremely small and produced a microbiocidal surface active under
384 visible (white) light conditions. The coating was shown to be effective against *S. aureus*, *S. aureus*
385 (MRSA), *C. difficile*, *E. coli*, *bacteriophage X174*, and *C. albicans*, but exhibited a greater photo
386 killing ability for Gram (+) bacteria.

387 Rose Bengal has been linked to synthetic polymeric supports such as silica [92], polystyrene (PS)
388 [64,93,94,95,96,97,98], Merrifield Resin [99] and polyethylene films with poly(vinylidene fluoride)
389 PVDF nanobeads [53].

390 The concept of inclusion of RB into a solid phase was raised in the 1970s [99, 96].
391 The first report of RB immobilized on a surface was by Shaap [99] in 1975 who linked RB by
392 covalent bonds to Merrifield Resin, a co-polymer consisting of styrene and divinylbenzene.
393 Studies of singlet oxygen production found that the immobilized photosensitizer had a lower rate of
394 singlet oxygen generation, due most likely to diffusion problems.
395 Bezman et al. in 1978 [96] first showed the photokilling ability of RB-PS nanoparticles towards *E.*
396 *coli*, which was reported to be effective in killing 99.99% of *E. coli* in a contaminated water sample
397 after 1-2 h exposure to white light.
398 Since polystyrene is considered to be a commonly available and low-cost material, RB was
399 immobilized on polystyrene porous films of cationically functionalized 2% DVB-crosslinked
400 polystyrene beads [95].
401 Nakonechny et al. [94] immobilized MB and RB on polystyrene by casting in chloroform and
402 subsequent air evaporation. The films were shown to have a porous structure with pores ranging
403 from 1 to 3 μm . Bacterial cells grew well on the surface of polystyrene and some of them even
404 starting to develop biofilms for a stronger attachment to the polystyrene surface. After 3 h under
405 illumination with white light in the presence of the immobilized RB the concentrations of *S. aureus*
406 and of *E. coli* dropped by 3 log and by 2.5 log respectively when using bacterial cells at a
407 concentration of 10^4 cells mL^{-1} . Under the same experimental conditions, immobilized MB
408 demonstrated lower efficiency than RB for both *S. aureus* and *E. coli*.
409 Recently, RB was immobilized onto a honeycomb film [93] made of poly(styrene-4-vinylbenzyl
410 chloride) (*ca.* 20 000 g mol^{-1} molar mass, with a low 1.2 dispersity) formed by nitroxide-mediated
411 radical polymerization. Rose Bengal was introduced subsequently by grafting through nucleophilic
412 substitution.
413 The porous polymer film, with a 2 – 2.5 μm diameter and a well-organized hexagonal patterned
414 surface, was more efficient for oxidation of organic molecules *via* singlet oxygen production at a
415 liquid/solid interface when compared with the corresponding non-porous flat films, revealing
416 promising PACT potential.
417 Nanoparticles surfaces modified with photosensitizer have also been proposed to enhance
418 antimicrobial activity of free RB [92].
419 Rose Bengal was used in silica nanoparticles to inactivate the Gram (+) bacteria, *S. epidermis* and *S.*
420 *aureus* (MRSA) [92].
421 The transparent silica nanoparticles functionalized with amine groups ($\text{SiO}_2\text{-NH}_2$), were prepared
422 by hydrolysis of TEOS in a reverse micro-emulsion method, functionalized with amino groups then
423 covalently attached to RB using EDC in MES buffer (pH = 6).

424 $\text{SiO}_2\text{-NH}_2\text{-RB}$ were shown to be more potent than free RB at inactivating Gram (+) bacteria.
425 The same conjugate was reported to have a singlet oxygen quantum yield lower than free RB (0.60
426 vs 0.75). Nevertheless, this value is higher than 0.43 previously obtained for RB bound to micron-
427 size polymer beads [99]. This suggest that nanoparticles increase the surface area making easier the
428 access of RB to the molecular oxygen present in the solution, thus increasing the damage to the
429 bacterial cells.

430 Overall, it appears that RB is a good candidate for PACT applications because it's commercially
431 available at high purity. Furthermore its carboxylate function, through a nucleophilic substitution,
432 allows the formations of covalent bonds between the inert support and the dye, resulting in
433 antimicrobial materials that may show more stability. On the other hand, the anionic character
434 might decrease the antibacterial activity spectrum. The conjugation of the anionic dye to
435 polycationic polymers such as chitosan seems to be an interesting approach to improve antibacterial
436 efficacy. Also the use of porous materials might improve increases the accessibility of the lethal
437 ROS to the target microorganisms.

438 5. Phthalocyanines

439 Phthalocyanines (Pc) are extended macrocyclic systems that have provoked significant interest in
440 PACT. Cationic water soluble phthalocyanines were shown to be active against Gram (–) *E. coli*
441 [100], *P. aeruginosa* [100,101,102] Gram (+) *S. aureus* (MRSA) [101,102], *E. faecalis* [102] and
442 the fungi *C. albicans* [101,102,103]. Chen et al. [104] demonstrated that poly-cationic lysine
443 moieties used as support for zinc phthalocyanine were active against Gram (+) and Gram (–)
444 bacteria, both *in vitro* and *in vivo*. The presence of a positive charge appears to promote a tight
445 electrostatic interaction with negative charges on lipopolysaccharides at the outer surface of Gram
446 (–) bacteria.

447 Recently, polymeric fibers doped with phthalocyanines were applied for the fabrication of
448 photoantimicrobial surfaces using the electrospinning technique [105,106,107,108,109].

449 Electrospinning has proven to be a relatively simple and versatile method for forming non-woven
450 fibrous mats with a defined porosity and water permeability with a very high fraction of surface
451 available to interact with cells. The possibility to host a variety of molecules to fine-tune their
452 properties for specific applications, together with the possibility to modify the structure, the
453 chemical and mechanical stability, and the functionality, makes this method appealing for
454 antimicrobial applications [110]

455 Following the photodegradation of Orange-G, Modisha et al. [111] confirmed that electrospun
456 conjugates of (2,3,9,10,16,17,23,24-octacarboxyphthalocyaninato)zinc(II) with magnetic
457 nanoparticles in polyamide-6 (PA-6) fibers were able to generate singlet oxygen after the
458 electrospinning process and Tombe [107] reported singlet oxygen quantum yields of 0.28 and 0.13
459 for a (4,11,18,25-tetrabenzylphthalocyaninato)zinc(II)-gold nanoparticle conjugate immobilized on
460 electrospun polystyrene fibers with and without gold atoms, respectively. The immobilized
461 conjugate was active as a photocatalyst for oxidizing organic pollutants, such as 4-chlorophenol and
462 Orange G using oxygen as an oxidant. Interestingly, Goethals et al. [112] reported that PA-6
463 membranes functionalized with [2,9,16,23-tetra(2-thioquinoline)phthalocyaninato]zinc(II) after the
464 electrospinning deposition were capable of photobleaching significantly more DPBF than
465 membranes that were non functionalized.

466 Polystyrene electrospun fibers were also employed as they have extensive π – π electronic
467 interactions between the aromatic systems of the phthalocyanine and the polymer
468 [105,106,107,108].

469 Masilela et al. [106] first reported the antimicrobial photo-inhibitory activity of a series of Zn(II)
470 phthalocyanines incorporated into electro-spun polystyrene fibers. The biocidal effect of
471 asymmetrical versus symmetrical substitution on the phthalocyanines was investigated using *S.*

472 *aureus*. All the unsymmetrically substituted complexes showed antimicrobial activity towards *S.*
473 *aureus* under illumination with visible light. The symmetrical (phthalocyaninato)zinc(II) (ZnPc)
474 and its symmetrical tetracarboxy derivative [2,9,16,23-tetra(4-
475 carboxyphenoxy)phthalocyaninato]zinc(II) showed no activity under illumination with light in the
476 fiber matrix due to low levels of singlet oxygen production.

477 Since heavy metals are expected to increase singlet oxygen quantum yield through enhanced
478 intersystem crossing, as a result of the heavy atom effect, Osifeko [105] incorporated into
479 polystyrene electrospun fibers low symmetry Pcs (i.e. mono substituted), including [2,9,16,23-
480 tetra(4-pyridyloxy)phthalocyaninato]lead(II) (PbTpyPc) and its tetracationic derivative [2,9,16,23-
481 tetra(4-*N*-methylpyridyloxy)phthalocyaninato]lead(II).

482 The tetracationic electrospun photosensitizer exhibited better singlet oxygen quantum yield and
483 improved inactivation response against *E. coli*, compared to the neutral precursor. Similarly, when
484 the tetracationic conjugate was tested, it was found to be more active than the non-ionic precursor as
485 no colony was observed on the agar plates after 30 minutes of irradiation with white light. Since
486 leaching studies revealed that the phthalocyanines are not released from the fibers, the authors
487 concluded that Pb doesn't result in additional toxicity.

488 Alternatively, Mosinger used polyurethane (PUR) electrospun nanofibers as the polymeric support
489 for incorporation of unsubstituted ZnPc [108].

490 Zinc phthalocyanine was revealed to be an efficient photooxidizing substrate. When exposed to
491 white light for 30 minutes, electrospun PUR-ZnPc doped nanofibers were able to kill *E. coli*,
492 however better results were obtained with polyurethane nanofibers doped with 5,10,15,20-
493 tetraphenylporphyrin (TPP).

494 Artarsky et al. also investigated the use of zinc phthalocyanines for PACT [113]. In this particular
495 example two different phthalocyanine compounds, [2,9,16,23-tetra(4-
496 *tert*butyl)phthalocyaninato]zinc(II) (TBZnPc) and (2,9,16,23-tetrasuphoxyphthalocyaninato)zinc(II)
497 (ZnPcTS) were entrapped into a silicate matrix prepared from tetraethylorthosilicate (TEOS) by the
498 sol-gel method.

499 The tetracationic ZnPcTS conjugate demonstrated more effective singlet oxygen production than
500 the neutral TBZnPc conjugate.

501 The photobactericidal results confirmed that the tetracationic ZnPcTS was more effective than the
502 neutral TBZnPc in killing *E. coli* in microbially polluted waters (*E. coli* reductions of about 1 log
503 after 120 minutes of exposure)

504 The authors hypothesized that ZnPcTS, being the dye with the more pronounced hydrophilic
505 character is likely to be preferentially deposited near the sol-gel surface, where the hydrophilic

506 character is prevailing and thus not evenly distributed throughout the whole bulk, while the tertiary
507 butyl derivative (TBZnPc) is mainly present in the internal parts of the matrix as a result of which it
508 is less accessible and therefore less active.

509 Phthalocyanines have been immobilized on a polymeric cellulose diacetate film [114] by co-
510 dissolution and casting or covalent attachment to a membrane [115] of chitosan, and used in a
511 circulating water photoreactor system as a model for a large-scale water-flow system [115].

512 For this purpose chitosan membranes were found to be very brittle, but their flexibility was
513 improved by casting the polymer into a nylon support, which offered flexibility without altering the
514 final transparency or translucency of the membranes.

515 The concentration of the (2,9,16,23-tetrasuphoxypthalocyaninato)zinc(II) as tetrasodium salt
516 (ZnPcS) covalently attached to the membrane was roughly estimated as $9 \mu\text{g cm}^{-2}$ based on solution
517 molar absorbance.

518 Photoantimicrobial activity was observed for the reinforced zinc phthalocyanine/chitosan
519 membrane after 35 mins with a $0.90 \times 10^{-5} \text{cfu ml}^{-1}$ cell count (initial cell count was $1.99 \times 10^{-5} \text{cfu ml}^{-1}$)
520 ¹) that dropped to $8.3 \times 10^2 \text{cfu ml}^{-1}$, showing a bacterial kill of $>2 \text{ log}$ in 160 min. Interestingly, the
521 same membrane, kept in the dark, after 9 months still showed a detectable activity with a reduction
522 of approximately 1 log of bacteria after 160 min, reflecting the thermodynamic stability of the
523 phthalocyanine system.

524 Pcs have shown to be promising candidate for the development of new antibacterial materials. The
525 possibility to make them positively charged with an appropriate choice of the substituent is an
526 interesting feature that is making them suitable starting materials for the development of new
527 photokilling surfaces. The efficient immobilization of Pc onto solid support and the stability that
528 those materials seem to have help to reduce the cost through an efficient recycling.

529 **6. Porphyrins immobilized on Natural Polymers**

530 Porphyrins have been linked to natural polymers for multiple purposes, for example they have been
531 bound to cellotriose moieties for optoelectronics purposes [116] and they have been conjugated to
532 chitosan to enhance gene transfection using PDT [117].

533 Commercially available protoporphyrin IX (PPIX) was successfully attached to nanoparticles
534 composed of an iron oxide core coated with dextran by an esterification reaction using 1,1'-
535 carbonyldiimidazole (CDI: 2 eq./porphyrin) as the electrophilic activator. These particles were
536 incorporated into cultured cancer cell lines showing a potential application in PDT [118].

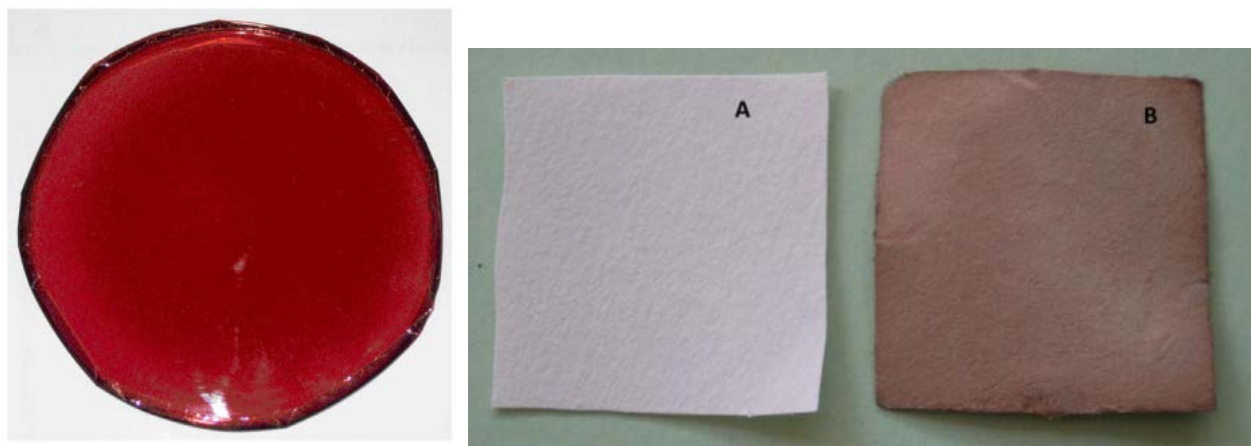
537 Organized, multilayer organic–inorganic films of sulfonated C₆₀, 5,10,15,20-tetra(4-*N*-
538 methylpyridyl)porphyrin (TMePyP⁴⁺) and chitosan were formed using electrostatic layer-by-layer
539 (LBL) assembly technology, which has proved to be a facile method for generating a wide range of
540 organized and stable thin films [119].

541 Porphyrin-based photobactericidal materials have been developed by grafting porphyrin-based
542 compounds onto natural polymers, such as chitosan [114,115] cellulose [120,121,122,
543 123,124,125,126,127,128,129] and dextran [118].

544 Porphyrins have been immobilized on polymeric cellulose diacetate films [114] or incorporated into
545 translucent reinforced nylon chitosan membranes by adsorption using 5,10,15,20-tetra(4-
546 hydroxyphenyl)porphyrin, (p-THPP) or by dissolution and casting with 5,10,15,20-tetra(4-
547 aminophenyl)porphyrin, (p-TAPP) and used in a circulating water photoreactor system as a model
548 for a large-scale water-flow system [115]. The concentration of the adsorbed porphyrin was
549 estimated to be about 5.7 μg cm⁻² while the concentration of the porphyrin immobilized by casting
550 was found to be 7.5 μg cm⁻² based on solution molar absorbances or on the weight of porphyrin
551 added, respectively.

552 When tested on *E. coli*, both p-THPP/chitosan and p-TAPP/chitosan membranes displayed a
553 photokilling ability after 40 mins of white light irradiation.

554 Neutral, anionic, and cationic porphyrins were covalently linked to cotton fabric [120,121,122] as
555 well as to cellulose esters [123,124,125] (Fig. 5) and were able to confer photobactericidal activity
556 on the cellulosic materials.



557
 558 **Fig. 5.** (Left) Porphyrinated cellulose laurate plastic film of 0.52% PPIX content [123].
 559 (Right) Photographs of (A) filter paper and (B) filter paper after reaction with aminoporphyrin and
 560 cyanuric chloride [129].

561 Protoporphyrin IX (PPIX) [123], 5,10,15-tri(4-methylphenyl)-20-(4-methylpyridyl)porphyrin [124]
 562 and porphyrins with a spacer arms comprising 4- or 11-carbons such as 5-[4-(3-
 563 carboxypropyloxy)phenyl]-10,15,20-tri(4-methylphenyl) porphyrin) and 5-[4-(10-
 564 carboxydecanoxy)phenyl]-10,15,20-tri(4-methylphenyl) porphyrin [125] were covalently attached
 565 to cellulose laurate esters films by a “one-pot, two-step” esterification reaction starting from
 566 cellulose and porphyrin.

567 PPIX [123] was covalently bound to the cellulose using Tosyl chloride and pyridine in
 568 dimethylacetamide/lithium chloride (DMA/LiCl) as binary solvent followed by esterification of the
 569 remaining carboxylic groups of cellulose by lauric acid in the same binary solvent system. This
 570 synthetic procedure allowed the dissolution and chemical modification of cellulose, a natural
 571 polymer having stiff, shape-stable structure into a plastic material allowing also the incorporation of
 572 the PPIX through a covalent bond. Seven porphyrinated films with different PPIX contents from
 573 0.19% to 1.1% were obtained by casting in a glass Petri dish (Fig. 5.)

574 No surviving colonies, for both *S. aureus* and *E. coli*, were seen for films with a porphyrin content
 575 of 0.52 or higher for PPIX [123], 0.35 for the cationic porphyrin 5,10,15-tri(4-methylphenyl),20-
 576 mono(4-*N*-methylpyridyl)porphyrin [124] and 0.18 and 0.30 for the porphyrins with the 4- or 11-
 577 carbons spacer arms, respectively [125].

578 Ringot et al. [120,122] used the Cu(I) catalyzed Huisgen 1, 3-dipolar cycloaddition or “click
 579 reaction” to covalently graft anionic, neutral, and cationic amino porphyrins on cotton fabric,
 580 without previous chemical modification of the cellulosic support.

581 Previously, the same group reported a direct cellulose azidation, followed by a “click” reaction in
 582 THF and water with acetylenic porphyrins [122].

583 5-(4-aminophenyl)-10,15,20-triphenylporphyrin (TPP-NH₂), anionic 5-(4-aminophenyl)-10,15,20-
584 tri(4-sulphonatophenyl)porphyrin (TPPS-NH₂) and cationic 5-(4-methylpyridyl)-10,20-di(2,4,6-
585 trimethylphenyl)-15-(4-aminophenyl)porphyrin (trans-MePy-NH₂) were grafted to cotton fabric
586 (3.5 x 3.5 cm, 0.27 g) using cyanuric chloride [120,121].

587 The highly reactive porphyrin with triazine link was characterized after the complete substitution of
588 the chlorine atoms with the use of piperidine (for neutral and cationic products) and sodium
589 sulfanilate (for the anionic compound) [121].

590 The modified fabric was non-toxic towards either bacterial species in the dark. After 24 h exposure
591 to white light irradiation, all modified surfaces caused a photobactericidal effect in Gram (+)
592 bacteria *S. aureus*. Cationic cotton gave the best result in terms of bacterial growth inhibition,
593 followed by neutral cotton and anionic cotton, percentages of bacterial growth inhibition were
594 100% for cationic cotton, 93.7% for neutral cotton and 37% for anionic cotton, respectively [120].

595 Following a similar approach, Mbakidi et al. [129] developed a novel antimicrobial paper by
596 grafting the tricationic porphyrin 5-(4-aminophenyl)-10,15,20-tri(4-*N*-methylpyridyl)porphyrin
597 using the same 1,3,5- triazine derivative described before (Fig. 5).

598 The porphyrin grafted paper was characterized using diffuse reflectance UV-Vis.

599 Results have showed a grafting yield of 55% (0.03 μmol/mg of paper sample), which was similar
600 with grafting yields of different porphyrins on cotton fabrics [120].

601 The photobiocidal activity of the photoantimicrobial filter paper was tested against *E. coli* and *S.*
602 *aureus*. After 24 hours exposure to white light at a fluence of 9.5 J/cm², no surviving bacteria were
603 detected on the grafted filter paper.

604 While there are several studies of porphyrins immobilized onto cellulosic materials (cotton fabrics,
605 microcrystalline cellulose) or cellulose strands, there have been few studies that describe the
606 covalent bonding of a porphyrin derivative onto a nanocrystalline cellulose (CNC) scaffold and its
607 use as photokilling surface [126,127].

608 Carpenter [127] and Feese [126] both used nanocrystalline cellulose (CNC) as the support for a
609 photobactericidal material formed from the covalent attachment of a [5,10,15-tri(4-*N*-
610 methylpyridyl)-20-(4-alkylphenyl)porphyrinato]zinc(II) to the surface of an azide-modified
611 cellulose nanocrystals through a “click” reaction.

612 Nanocrystalline cellulose (CNC) is obtained from cotton fiber through the acid hydrolytic
613 disruption of the amorphous domains of cellulose and the consequent conversion of native cellulose
614 fibers into a colloidal dispersion. Due to its good properties such as large surface area, good
615 mechanical strength and biodegradability, as well as availability and biodegradability, it is currently
616 being investigated as a component of transparent flexible films.

617 The photobactericidal activity of porphyrin–cellulose nanocrystals films was investigated against a
618 wide variety of bacteria, such as *A. baumannii*, multidrug-resistant *A. baumannii* (MDRAB),
619 methicillin-resistant *S. aureus* (MRSA), *P. aeruginosa* [127], *E. coli*, *S. aureus* and *M. smegmatis*
620 (mycobacterium) [126].

621 Gram (+) positive *S. aureus*, *S. aureus* (MRSA), Gram (–) *A. baumannii* and *A. baumannii*
622 (MDRAB) gave a reduction in colony forming units (CFUs) even after 15 min illumination with
623 white light.

624 *P. aeruginosa* appeared to be susceptible to photodynamic inactivation with no statistically
625 significant inactivation observed when incubated for less than 30 min. For all the bacterial strains
626 examined a 30 min light dose achieved a reduction in viable cells greater than a 15 min light dose,
627 attributable to the higher amount of cytotoxic reactive oxygen species formed, in particular $^1\text{O}_2$.

628 Since confocal laser scanning microscopy after incubation with *S. aureus* suggested a lack of
629 internalization of the Ps, this study also suggested that reactive oxygen species produced
630 extracellularly by photodynamic therapy can be effective without internalization of the
631 photosensitizer.

632 It has been shown that porphyrins keep their antimicrobial properties when grafted to natural
633 polymers, such as chitosan or cellulose or dextran. These modified polymers have been casted into
634 photobactericidal membranes or films or used as cotton textiles to form eco-friendly materials with
635 potential industrial, medical, and household applications.

636 The field still faces with the key challenge of having a photobactericidal material with significant
637 activity and with the dye present at the lowest concentration as possible, minimizing the leaching
638 and with an improved durability of the material.

639 **7. Porphyrins linked to synthetic polymers**

640 Porphyrins, due to their versatile nature, have been linked to a great variety of synthetic polymers.
641 Water-soluble, [5,10,15,20-tetra(4-sulphophenyl)porphyrinato]iron(III) was effectively immobilized
642 into anionic Dowex resin for catalytic purposes. By having a suspension of the Dowex resin in
643 distilled water with 4 mg of the iron(III) porphyrin and stirred for 2-3 hours at room temperature,
644 the attachment of the porphyrin was followed due to the surface changing color and becoming green
645 [130]. This system was stable, in fact even after filtration and washing with distilled water, the solid
646 was found to retain completely the adsorbed iron porphyrin, and it was easily recovered after the
647 reaction and reused without loss of activity.

648 Similar results were obtained with Mn(II) porphyrins supported on commercially available resins
649 [131].

650 Ribeiro et al. [132] studied the photocatalytic behavior of porphyrins covalently linked to a
651 Merrifield polymer previously modified with an excess of α , ω -diamines to obtain the
652 aminoalkylated polymers, making them suitable for reaction with chlorosulfonated porphyrins. The
653 authors also reacted the chlorosulfonyl porphyrin with commercially available aminomethylated
654 polystyrene divinylbenzene co-polymer to obtain a porphyrin covalently linked to the polymer but
655 close in proximity to the polymer backbone due to the absence of a spacer molecule. This conjugate
656 was found to have the highest value of porphyrin incorporated. All of the supported photosensitizers
657 were able to generate singlet oxygen with an efficiency dependent on the structure of the spacer
658 between porphyrin and polymer. The catalyst was filtered, washed and dried and could be recycled
659 with a new substrate batch, with one of the catalysts being reused for three catalytic cycles.

660 Water-soluble Pd(II), Pt(II) and Rh(III) complexes with 5,10,15,20-tetra(4-*N*-methylpyridyl)
661 porphyrin (TMPyP⁴⁺) and 5,10,15,20-tetra-(4-*N,N,N*-trimethylaminophenyl)porphyrin were
662 immobilized in per-fluorinated ion-exchange membranes (e.g. Nafion®) after boiling in
663 concentrated nitric acid for 30 min and in double distilled water for 30 min to clean them and to
664 make them optically transparent above 240 nm [133]. The membranes revealed a good
665 photostability and high oxygen permeability.

666 [5-(4-hydroxyphenyl)-10,15,20-tris(4-sulfonatophenyl)porphyrinato]zinc(II) and [5-(4-
667 hydroxyphenyl)-10,15,20-tris(4-*N*-methylpyridyl)porphyrinato]zinc(II) were transesterified on
668 transparent poly (methylmethacrylate) polymer films in toluene in the presence of *p*-toluenesulfonic
669 acid [134]. Related to the number of methyl esters present in the PMMA, the concentration of the
670 porphyrins in the polymer was found to only be 1%.

671 Xing et al. [135] described the complex formed by electrostatic interactions of water-soluble
672 anionic polythiophene with tetracationic 5,10,15,20-tetra[4-(6-*N,N,N*-
673 trimethylammoniumhexyloxy)phenyl]porphyrin bromide (TPPN). This electrostatic complex
674 adsorbed Gram (-) and Gram (+) bacteria and generated singlet oxygen effectively to kill the
675 bacteria under white light. In this case, the photokilling ability of the system was tested against *E.*
676 *coli* and *B. subtilis*, for which ca. 70% and 90% of bacterial viability reduction, respectively, was
677 observed after only 5 min of irradiation with white light at a fluence rate of 90 mW cm⁻².

678 Doped polysilsesquioxane films were synthesized adding the anionic 5-(4-carboxyphenyl)-
679 10,15,20-tris(4-methylphenyl)porphyrin at different concentrations in THF/water using an
680 appropriate amount of formic acid as catalyst [136]. The final concentrations were 2.6 x10⁻⁴ w / w
681 and 5.2 x10⁻⁴ w / w respectively.

682 Bridged silsesquioxanes allowed the creation of a moldable, versatile and flexible material at room
683 temperature, which could be used for the dispersion of dyes.

684 *In vitro* investigations showed that they were able to kill *C. albicans* upon irradiation with visible
685 light. The doped films produced a ~2.5 log decrease in *C. albicans* (99.7 % cellular inactivation)
686 after 60 min irradiation, but 96% cellular inactivation was observed after 30 minutes irradiation.
687 When tested under conditions of microbial growth, yeast cells exposed to the film and illuminated,
688 showed growth delay compared with controls. The free form of photosensitizer was evaluated as
689 well and it was found to have a small photoinactivation effect of 0.5 log decrease after 60 mins.
690 5,10,15,20-tetra(4-*N,N*-diphenylaminophenyl)porphyrin and its Pd(II) complex immobilized on
691 optically transparent indium tin oxide (ITO) electrodes have been proposed to inactivate *C. albicans*
692 cells for possible applications in the control and disinfection of the aqueous suspension of
693 microorganisms [137].
694 These films exhibited a photosensitizing activity causing a ~3 log decrease (99.9 % cellular
695 inactivation) of *E. coli* after 30 minutes and ~2.0 log decrease (99.7%) of *C. albicans* survival after
696 60 minutes, suggesting that eukaryotic cells are more difficult to inactivate than bacteria.
697 As before [136] yeast cells showed growth delay compared with controls when tested under
698 condition of microbial growth.
699 Banerjee et al. [138] described the covalent functionalization of carbon nanotubes with porphyrins
700 for antiviral purposes. PPIX was immobilized onto nanomaterial scaffolds such as multi-walled
701 carbon nanotubes (MWNTs) to develop antimicrobial nanocomposite films by combining the
702 biocidal ability of porphyrins with the mechanical strength of the nanotubes.
703 A treatment with 1000 $\mu\text{g mL}^{-1}$ of the porphyrin-nanotube conjugate caused more than a 250-fold
704 reduction in the effective infectious Influenza A viral dose after a 30 min exposure to visible light.
705 Both the conjugated and the unconjugated MWNTs were incubated in the dark and in both cases
706 there was no observable photokilling effect.
707 Since carbon nanotubes can be easily recovered by filtration making them appealing for possible
708 reuse of the material, the authors showed that the conjugate can indeed be recovered and reused and
709 it still effectively causes a 50-fold reduction in the infectious viral dose, even after five uses.
710 In previous work [139], the same porphyrin-nanotube conjugate showed a high bactericidal activity
711 against *S. aureus* cells upon irradiation with visible light. In fact the MWNT - PPIX conjugate, after
712 coating on nitrocellulose filter membranes, was able to inactivate more than 80% of the bacterial
713 colonies after 1 h exposure to visible light.
714 Gao et al. investigated the use of cross-linked polystyrene (CPS) microspheres (0.32 - 0.45 μm in
715 diameter), with a cross-linking degree of 4% for the direct synthesis of a porphyrin-polystyrene
716 conjugate through modification of the polystyrene microspheres themselves [140].

717 CPS are readily available, cheap, mechanically robust and chemically inert and they can undergo
718 facile functionalization.

719 Pyridylporphyrin (PyP) was synthesized directly on the surface of chloromethylated crosslinked
720 polystyrene microspheres (CMCPS microspheres).

721 Pyridinecarboxaldehyde groups were introduced through a quaternization reaction to form the
722 modified microspheres (PyAL-CPS). Finally, PyAL-CPS microspheres were condensed with
723 pyrrole and free 4-pyridinecarboxaldehyde using the Alder reaction to form the porphyrin *in situ*.

724 PyP-CPS microspheres were reacted with CH₃I as the quaternization reagent, to obtain the cationic
725 analogue. In other papers [141,142] 4-hydroxybenzaldehyde (HBA)-bound CPS microspheres,
726 pyrrole, and benzaldehyde were condensed similarly, again using the Adler reaction.

727 Two different methods of analysis allowed confirmation of the attachment of the porphyrin to the
728 microsphere. Through IR spectroscopy it was possible to confirm attachment of the porphyrin to the
729 microsphere, while UV-visible spectroscopy confirmed the presence of the Soret and Q-bands of
730 the porphyrin molecules.

731 Interestingly, in previous papers [141,142], the amount of porphyrin immobilized on the
732 microsphere surface was determined through complexation of the immobilized porphyrin with zinc
733 (ZnCl₂ solution) followed by analysis of Zn ion content in the final solution using EDTA through a
734 complexometric reaction.

735 Griesbeck et al. [143] more recently reported polymer-bound sensitizer systems using TPP or
736 5,10,15,20-tetra(4-methylphenyl)porphyrin (TTP). Commercially available polystyrene beads
737 (approx. 60 μm) cross-linked with divinylbenzene were utilized as the polymeric support.

738 The PS beads were loaded with the sensitizing molecule by swelling with a solution of catalytic
739 amounts of TPP and TTP in ethylacetate followed by evaporation of excess solvent from the
740 solution. Following this photooxidation of β-pinene and ethyl tiglate was used to quantify
741 photoactivity of the porphyrin loaded beads. The authors were able to show that singlet oxygen is
742 produced in a solvent-free photooxygenation process.

743 Recently Griesbeck et al. designed a solventless reaction which has been the subject of considerable
744 interest as an eco friendly synthetic approach, reducing the amount of environmentally problematic
745 and expensive solvents and retarding the production of side products as a result of the enhanced
746 selectivity [144].

747 Commercially available PPIX and 5,10,15,20-tetra(4-vinylphenyl)porphyrin (TSP) were attached
748 to polystyrene beads cross-linked with divinylbenzene. The process was carried out using emulsifier
749 free polymerization of styrene with divinyl benzene for the formation of nanosized polystyrene-
750 divinylbenzene particles. The method was a one-pot synthetic method with the porphyrin embedded

751 in the backbone of the polymer. This technique allowed the syntheses of the translucent particles in
752 a simple and reproducible way.

753 In particular, the production of singlet oxygen under irradiation conditions was of interest from the
754 viewpoint of PACT.

755 Inbaraj et al. [145] reported the functionalization of cationic N-alkylpyridinium polystyrene
756 supports with 5,10,15,20-tetra(4-sodiumsulphonatophenyl)porphyrin (TPPS) and its metallo
757 complexes [5,10,15,20-tetra(4-sodiumsulphonatophenyl)porphyrinato]cadmium(II) (CdTPPS) and
758 [5,10,15,20-tetra(4-sodiumsulphonatophenyl)porphyrinato]zinc(II) (ZnTPPS). Since the polymeric
759 support used was 2% cross-linked divinylbenzene with styrene, the porphyrin molecule was
760 attached by ionic interactions from a pyridine to the sulfonate group on the porphyrin. *N,N*-
761 dimethyl-4-nitrosoaniline (RNO) was used as an indicator for photo-induced singlet oxygen with
762 imidazole as a chemical trap for singlet oxygen. Quantum yields were reported as 0.29, 0.27, and
763 0.16 for PS-H₂TPPS, PS-ZnTPPS, and PS-CdTPPS, respectively, whilst the unbound porphyrins
764 had singlet oxygen quantum yields of 0.62 and 0.81 for H₂TPPS and ZnTPPS, respectively. The
765 binding of the porphyrin to the polymer was found to decrease the quantum yield. The authors
766 attributed this to structural deformation of the appended porphyrins on the spherical shape of
767 polymer bead surface, and the resulting decrease in exposition to light.

768 TTPS and their metalloderivatives [MTPPS; M=Cu(II), Zn(II), Ag(II), and Cd(II)] immobilized on
769 a support made of poly(4-vinylpyridine) (PVP), crosslinked and linear polystyrenes partially
770 chloromethylated and quaternized, and polyethylene glycol (PEG) have demonstrated their ability
771 to carry out enzyme mimetic reactions efficiently [146].

772 Recently, the commercial hydrophilic [5,10,15,20-tetra(4-
773 sodiumsulphonatophenyl)porphyrinato]manganese(III) chloride (MnTPPS) was mixed with
774 dimethyldioctadecyl-ammonium bromide (DODMABr) to form a hydrophobic complex that was
775 used to construct microporous honeycomb films (MHFs) on glass substrates *via* casting an organic
776 solution of MnTPPS-DODMA at relative humidities higher than 80% [147].

777 PS was used to increase the strength of the film but also to modulate the pore sizes.

778 The porous polymer film, 800 nm in diameter and a well-organized hexagonal patterned surface,
779 was more efficient for oxidation of organic molecules *via* singlet oxygen production when
780 compared with the corresponding non-porous thin films. This is in agreement with results by
781 Pessoni et al. [93].

782 These microporous honeycomb films of MnTPPS-DODMA were shown to have more efficient
783 antibacterial activity when compared with MnTPPS-DODMA non-porous thin films (83%
784 reduction versus 43% respectively) upon irradiation with visible light for 1 h. Bacterial reduction in

785 the dark was 7%, showing a direct correlation between irradiation with light and photokilling ability
786 of the substrate.

787 Magaraggia et al.[148] encapsulated an hydrophilic porphyrin into silica microparticles prepared by
788 the Stöber method through the ammonia-catalyzed hydrolysis of TEOS to form a conjugate with a
789 mean particle diameter of ca. 0.9 μm .

790 Limited photobleaching of the encapsulated porphyrin was carried out when the porphyrin was
791 exposed to visible light. The microparticles exhibited a photosensitizing activity causing a decrease
792 in survival by a 4 log reduction after a 20 min irradiation of the Gram (+) bacterium *S. aureus*
793 (MRSA), and a 30 min irradiation of the Gram (-) *E. coli* in the presence of 10 μM of the porphyrin
794 silica microparticles.

795 Silica based nanomagneto-porphyrin hybrids were described by Alves [149] and Carvalho [150],
796 these materials were particularly appealing due to the possibility to easily isolate and purify them
797 using a magnetic field.

798 Carvalho et al. investigated the use of magnetic nanoparticles (Fe_2O_3 in this case) surrounded by a
799 silica shell for the attachment of porphyrins for use as antimicrobial agents. Characterization of the
800 nanoparticles was carried out using pXRD and UV-visible spectroscopy. The attachment was
801 monitored by UV-visible spectroscopy and showed that the relative amount of porphyrin attached
802 was 4 – 5% (w / w).

803 These new multicharged nanomagneto-porphyrin hybrids were very stable in water. The cationic
804 hybrids induced a total photoinactivation of *E. faecalis*, *E. coli*, and T4-like phage, even when used
805 at 20 μM , upon irradiation with white light of 21.6, 43.2, and 14.4 J cm^{-2} , respectively.

806 5-(2,3,4,5,6-pentafluorophenyl)-10,15,20-tripyridylporphyrin and the corresponding cationic
807 5,10,15-tri(4-*N*-methylpyridyl)-20-(2,3,4,5,6-pentafluorophenyl)porphyrins as tri-iodide salt were
808 grafted to cationized silica-coated magnetic nanoparticles of Fe_3O_4 and CoFe_2O_4 [149]. Their use
809 in PACT against the Gram (-) bacteria *A. fischeri* was investigated by monitoring the decrease in its
810 natural bioluminescence during the photosensitization process using a luminometer and monitoring
811 the photo-inactivation kinetics in real-time.

812 The cationic nanomagneto-porphyrin hybrids were found to be highly efficient at bacterial
813 inactivation and they also showed sustained photoinactivation over six cycles. It was also shown
814 that 2.5 h (150 min) was required to inactivate 7 log of bacteria (first cycle), but they could
815 cumulatively inactivate 42 log of bacteria in 21.5 h.

816 Porphyrins have been covalently linked to aminoalkylated silica particles by initial activation of the
817 porphyrin nucleus using chlorosulphonation [151].

818 Rychtarikova et al. [152] entrapped TMePyP⁴⁺ in microporous silica gels prepared by the sol-gel
819 method using tetrakis(2-hydroxyethoxy)silane (THES) and tetra methoxysilane (TMOS).
820 All the composites containing THES showed good adhesion to glass, and the THES composite
821 showed no shrinkage in three months, as well as being shape and volume stable in air for three
822 months. The main disadvantage of the composite is low mechanical and chemical stability.
823 All of the composites were particularly active against *E. coli* but, in general, THES composites
824 with lower specific surface areas were more effective than TMOS analogs, probably because the
825 PEG 600 improved the flexibility, and thus oxygen diffusion, in the gel.
826 Recently, nanofibre materials were developed with encapsulated porphyrinoid photosensitizers that
827 generate ¹O₂ in high quantum yields upon irradiation with visible light. The small diameter of the
828 nanofibres allowed the efficient diffusion of ¹O₂ outside the nanofibres to kill *E. coli*, *S. aureus* and
829 *P. aeruginosa*. bacteria [108,153,154,155].
830 Mosinger et al. utilized Polyurethane (PUR), TPP and its Zn(II) derivative (5,10,15,20-
831 tetraphenylporphyrinato)zinc(II) (ZnTPP) [108] to form nanofibrous layers 0.03 mm thick and
832 with 0.12 % TPP and 0.10 % ZnTPP content, respectively [108,153]. When exposed to light the
833 nanofabrics produce enough singlet oxygen to kill the bacteria cells. PUR, used as control without
834 the incorporated porphyrin sensitizers, either exposed to light or kept in the dark had no effect on
835 the bacterial growth.
836 The PUR nanofabrics have bactericidal effects at their surfaces, however free-base porphyrin TPP
837 showed better efficiency and photostability.
838 Electrospun nanofibres were prepared by doping polyurethane LarithaneTM (PUR),
839 polycaprolactone (PCL), polystyrene (PS) and polyamide 6 (PA6) with TPP with a final 1 wt %
840 TPP each [156,157].
841 The doped nanofibre textiles efficiently photo-generate ¹O₂. When tested against *E. coli*, after 60
842 minutes irradiation with white light, the PUR, PS, and PCL nanofibre materials exhibited
843 antibacterial activity and completely inhibited bacterial growth upon irradiation with visible light.
844 The PA6 nanofiber showed lower antibacterial activity probably due to lower production of ¹O₂.
845 Since metal nanoparticles have been reported to have antibacterial and antifungal properties,
846 Managa et al. [154] tested the antibacterial properties of the conjugate formed between [5,10,15,20-
847 tetra-(4-carboxyphenyl) porphyrinato]gallium(III)chloride (ClGaTCPP) and platinum nanoparticles
848 PtNPs in solution, and after immobilization onto electrospun styrene nanofibers. Gallium was
849 chosen as the central metal in this case because it enhances the intersystem crossing to the triplet
850 state thus improving singlet oxygen, this happens due to the size of gallium, in relation to the heavy
851 atom effect.

852 When tested in solution, the conjugate (ClGaTCPP)-PtNPs had an improved antibacterial activity
853 when compared to the nanoparticles alone, due to synergistic effects.

854 The doped nanofabrics, when irradiated with light, showed positive growth inhibition against *S.*
855 *aureus* when compared to those that were kept in the dark; there was also an enhanced effect for
856 ClGaTCPP–PtNPs, compared with ClGaTCPP.

857 Recently, Henke et al. [155] studied the influence of the wettability of the surfaces of TPP-PS
858 electrospun nanofibres on the antibacterial activity of *E. coli* on the surface of the electrospun
859 fibres.

860 Sulfonation, oxygen plasma treatment, and even the application of a thin polydopamine coating on
861 the surface of the polystyrene electrospun nanofibres strongly increased the
862 wettability/hydrophilicity of the hydrophobic polystyrene nanofibers, without causing damage to
863 the nanofibers, leakage of the photosensitizer, or any change in the spectral characteristics of TPP.
864 The increase in surface wettability resulted in acceleration of the photo oxidation of external
865 substrates, and an increase in the antibacterial activity of the nanofibres.

866 Sherrill et al. investigated the use of nylon films as supports for immobilization of PPIX and zinc
867 PPIX to create an antimicrobial material [158]. Nylon 6,6 was grafted *via* poly (acrylic acid) (PAA)
868 resulting in a surface coverage of 57%.

869 Grafting the two different porphyrin derivatives (PPIX and Zn-PPIX) resulted in nearly identical
870 values of surface coverage, approximately 36%, for both sample types, however, no biological
871 studies have been carried out on these surfaces to date.

872 Bozja et al. also investigated the use of nylon fibers as a support for porphyrin molecules [159]. The
873 samples were prepared in a similar way to that reported by Sherrill et al.

874 The PPIX-nylon conjugate efficiently killed more than 95% of *S. aureus* bacteria after a 30 minutes
875 exposure at a fluence of 60,000 lux, while no effect was observed with Gram (–) *E. coli*. The
876 ZnPPIX-nylon conjugate was revealed to be slightly more efficient against *E. coli*, with a 30% cell
877 killing using 60,000 lux after 30 min exposure. For the Gram (+) bacteria *S. aureus* 94% of bacteria
878 was killed using 40,000 lux. Overall the ZnPPIX was found to be more effective against both Gram
879 (+) *S. aureus* and Gram (–) *E. coli* bacteria.

880 The attachment of porphyrins to synthetic polymers have been extensively investigated. Since a lot
881 of polymers precursors are cheap and commercially available, this approach presents the advantage
882 of being cheaper than others previously analyzed. Some new photobactericidal materials offered the
883 possibility to be recovered and reused, making the materials very interesting for an eco friendly
884 approach.

885 **8. Others Photosensitizers**

886 Benabbou et al. [160] grafted or incorporated into inert solid supports an anthraquinone derivative,
887 9,10-anthraquinone 2-carboxylic acid (ANT) and a benzo-[b]triphenylene-9,14-dicarbonitrile
888 (DBTP), as they are known to be good singlet oxygen generators.

889 The ANT was converted to its triethoxysilyl derivative by condensation with APTES and grafted to
890 commercial silica beads (3–5 mm diameter, pore diameter ca. 9 nm), by reflux in toluene and was
891 shown to be more effective than the DBTP derivatives grafted on a commercial amino
892 functionalized silica powder (Si-NH₂ 40–63 μm particles) when tested against *E. coli*. This may
893 have been due to the higher photo-oxidation efficiency of ANT [161]. Both derivatives displayed a
894 good stability in aqueous suspension, with no leakage of the sensitizing molecule into the water.
895 Commercially available silica powders or beads were chosen because 9, 10-anthraquinone
896 immobilized on silica gel was found to be transparent [162].

897 Chen et al. studied the ability of chitosan to potentiate the activity of erythrosine (ER) against
898 bacteria and yeast through the preparation of nanoparticles by the ionic gelation method.

899 Comparing the PACT effect against erythrosine alone and chitosan alone, the combination of ER/
900 CS nanoparticles showed an enhanced antimicrobial effect against *S. mutans*, *P. aeruginosa* and *C.*
901 *albicans* [163].

902 Neutral and cationic pyrrolidine fused chlorins have also been investigated recently as potential
903 PACT agents when immobilized on 3-bromopropyl-functionalized silica and Merrifield resin [164].
904 Since it had been observed from the same research group that the efficiency in the photoinactivation
905 of *E. coli* was influenced by the number of charges on the final immobilized conjugate [165] further
906 treatments with 1-methylimidazole or pyridine were performed on silica gel and on Merrifield resin
907 to increase the number of positive charges on the surface of the material.

908 Overall, this study showed that the increased number of positive charges and their dispersion on the
909 surface of the materials strongly influences the photodynamic efficiency of the conjugate.

910 Silica with chlorin and Merrifield resin/chlorin in combination with pyridine showed the best
911 activity against *E. coli*.

912

913 **9. Conclusions**

914 PACT is a field of ongoing and active research to meet the urgent need to find alternative options
915 for microbial killing.

916 This technique is particularly appealing due to the possibility of using visible light (and possibly
917 sunlight) to inactivate microorganisms, the possibility to recycle and reuse the photosensitizers in an
918 eco friendly approach, and the lack of bacterial resistance induced in microorganisms.

919 Since the initial investigations in the 1970s many photosensitizers, including Methylene Blue,
920 Toluidine Bue, Rose Bengal, Ruthenium Complexes, Phthalocyanines and Porphyrins have been
921 immobilized onto a huge variety of supports, mostly natural or synthetic polymers, such as chitosan,
922 cellulose, cotton, polystyrene, polyurethane, nylon, but also silica beads, nanotubes.

923 Since currently available materials suffer of loss of antimicrobial activity by leaching of the biocide
924 with the potential risk of releasing hazardous agents in the media, PACT community should invest
925 in the development of new supports, and, most important, in the development of new ways to
926 immobilize photosensitizes on solid support to create new photokilling materials with the potential
927 capability of rapid efficient, and low-cost sterilization of a range of bacteria.

928 A stable and uniform surface coating would allow an high availability of the dye at the surface and
929 the most favorable conditions for the interaction with bacteria and with the oxygen naturally present
930 in the environment. Nevertheless this approach might be difficult due to the fact that sometimes is
931 difficult to have an uniform coating of the surface, leading with reproducibility problems. Embed
932 the dye in a porous support might be a promising alternative, proving that the oxygen must be able
933 to and interact with sensitizer and bacteria.

934 The leaching of the photosensitizer is a general problem that emerged frequently. Thus the
935 development of new ways to immobilize photosensitizes on solid support seems to be a key
936 challenge towards the practical application of solid-supported PACT devices.

937 The choice of the sensitizer (cationic/anionic) beside being a key factor going to influence the
938 bacterial strains activity of the solid-supported PACT device, need to be done taking into
939 considerations also other desiderables characteristics, such as an economic and easily scale up
940 synthesis.

941 The progress and the possible applications of those photosensitizing surfaces demonstrate that this
942 is a promising approach for the killing of bacteria, viruses and fungi.

943

944

945 *Acknowledgements*

946 The authors would like to thank the Sir Halley Stewart Trust for funding.

949 **Table 1.** Reports of photoinactivation of Gram (+) and Gram (-) bacteria and *in vitro*.

Ref	Ps	Support	Light type	Target organism	Fluence rate or Light Dose or lux	Period of illumination
[47]	MB	silicone	laser light (660 nm)	<i>S. epidermidis</i>	58 J cm ⁻² 117 J cm ⁻²	5 min every 30 min, 10 min every 60 min or 20 min every 120 min (6 h total)
[48]	MB	silicone elastomers	laser light (660 nm)	<i>E. coli</i> <i>S. epidermis</i>	19.5 J cm ⁻²	10 min
[49]	MB TBO	silicone polymer	laser light (634 nm)	<i>S. epidermis</i> <i>E. coli</i>	0.19 W cm ⁻² (TBO) 0.0325 W cm ⁻² (MB)	4 min (TBO) 21 min (MB)
[50]	MB	Silicone polymers	28-W BIAX 2D T5 compact fluorescent lamp, white light	<i>S. aureus</i> (MRSA)	2,305 lux	24 h
[51]	MB TBO	PUR	white light	<i>S. aureus</i>	2000 lux	24 h
[52]	TBO	PUR silicone polymers	laser light (634 nm)	<i>E. coli</i> <i>S. aureus</i> (MRSA)		2 min 3 min
[53]	RB, MB TBO	PVDF nanobeads on polyethylene film	luminescent lamp, white light	<i>S. aureus</i> <i>E. coli</i>	1.46 mW cm ⁻¹	3 h 24 h
[54]	TBO	cellulose acetate layer	white light	<i>S. aureus</i> <i>P. aeruginosa</i>	778 ± 12 lux	8 h 16 h 24 h
[55]	TBO RB	cellulose acetate	General Electric 28W Biax 2D compact fluorescent lamp, white light	<i>S. aureus</i> (MRSA) <i>E. coli</i> <i>C. albicans</i> <i>C. difficile</i> bacteriophage X174	3700 ± 20 lux	2 h 4 h 6 h 16 h
[56]	TBO RB	cellulose acetate	General Electric 28W Biax 2D compact fluorescent lamp white light	<i>S. aureus</i>	3700 ± 20 lux	6 h
[57]	MB	Silicone elastomers	laser light (660 nm)	<i>S. aureus</i> <i>E. coli</i>		5 min
[60]	TBO	CS	high Power LED 635±5 nm	<i>S aureus</i> <i>P. aeruginosa</i> <i>A. baumannii</i>	60 mW cm ⁻²	30 min
[61]	TBO	PMVE/MA copolymer	635 nm Paterson Lamp	<i>C. albicans</i>	100 mW cm ⁻² 100 J cm ⁻² 200 J cm ⁻²	
[62]	NMB	Urethane-acrylate Styrene-butadiene copolymers	Paterson lamp with filter at 615-645 nm	<i>S. epidermis</i> <i>E. coli</i>	11.5 J cm ⁻² 5.8 J cm ⁻² 2.9 J cm ⁻² 1.5 J cm ⁻²	0.5 min 1 min 2 min 4 min
[64]	MB RB Eosin	PS resin Silicagel Activated carbon	four cold white TLE 22 W23 Philips lamps	<i>E. coli</i>		10 min 20 min 30 min 40 min 60 min
[72]	Ru(II) phenantroline complexes Ru(II) bipyridyl complex	pSil	150 W Xe lamp or sunlight	<i>E. coli</i> <i>E. faecalis</i>	0.6 M J m ⁻² 0.8 M J m ⁻²	9 h
[73]	Ru(II) phenantroline complex-C60 fullerene	pSil	laboratory solar simulator-white light	<i>E. faecalis</i>	20 W m ⁻²	9 h
[74]	Ru(II) phenantroline complex	pSil	150 W Xe lamp and sunlight	<i>E. faecalis</i>	20 W m ⁻² 400 W m ⁻²	4h (Xe lamp) 60 min (sunlight)
[75]	Ru(II) complexes	pSil	150 W Xe lamp and sunlight	<i>E. faecalis</i>	400 W m ⁻²	9 h
[76]	Ru(II) phenantroline complex	pSil	sunlight	<i>E. coli</i>	0.6 M J m ⁻²	5 h

				<i>E. faecalis</i>	0.8 MJ m ⁻²	
[81]	RB	CS membrane	broad-spectrum Lumacare lamp with a 540 ± 15 nm filter (green light)	<i>E. faecalis</i>	5 J cm ⁻² 20 J cm ⁻² 40 J cm ⁻² 60 J cm ⁻²	
[82]	RB	chitosan	broad-spectrum Lumacare lamp with a 540 ± 15 nm filter (green light)	<i>E. faecalis</i>	5 J cm ⁻² 10 J cm ⁻²	1.66 min 3.33 min
[83]	RB	PDMS with chitosan on the surface	120 W incandescent lamp	<i>E. coli</i> <i>S. aureus</i>		60 min
[84]	RB	CS	broad-spectrum Lumacare lamp with a 540 ± 15 nm filter (green light)	<i>E. faecalis</i> <i>P. aeruginosa</i>	20 J cm ⁻² 40 J cm ⁻² 60 J cm ⁻²	15 min 30 min 60 min
[85]	RB	CS	broad-spectrum Lumacare lamp with a 540 ± 15 nm filter (green light)	<i>E. faecalis</i>	20 J cm ⁻² 40 J cm ⁻² 60 J cm ⁻²	
[92]	RB	silica nanoparticles	Lumacare lamp with a 525 nm bandpass filter	<i>S. aureus</i> (MRSA) <i>S. epidermis</i>	33 J cm ⁻²	40 min
[94]	RB MB	PS films	white luminescent lamp emitting in the range of 400 – 700 nm (visible light)	<i>S. aureus</i> <i>E. coli</i>	1-3 mW cm ⁻²	30 min 3 h
[96]	RB	PS beads	four 15 W Silvana Fluorescent Bulb	<i>E. coli</i>		
[105]	PbTpyPc and its tetracationic derivative [2,9,16,23-tetra(4- <i>N</i> -methylpyridyloxy)phthalocyaninato]lead(II)	Electrospun PS fibers	300 W lamp with 600 nm glass and water filters	<i>E. coli</i>		30 min
[106]	ZnPc	Electrospun PS fibers	300 W lamp with 600 nm glass and water filters visible light	<i>S. aureus</i>		90 min
[108]	ZnPc	Electrospun PUR fibers	150 W cold white light	<i>E. coli</i>		30 min
[113]	TBZnPc ZnPcTS	silicate matrix	Bonnett-Pell lamp with a maximum emission at 660 nm	<i>E. coli</i>	0.60 mW cm ⁻²	120 min
[115]	ZnPcS p-THPP p-TAPP	CS membrane	500 W halogen lamp	<i>E. coli</i>		90 min
[120]	TPP-NH ₂ TPPS-NH ₂ Trans(Me-Py+) NH ₂	cotton fabric	LED model Luxeon Star white Lambertian LXHL-MW1D 5500K) 400-800 nm (white light)	<i>S. aureus</i> <i>E. coli</i>	9.5 J cm ⁻²	24 h
[121]	TPP-NH ₂ TPPS-NH ₂ Trans(Me-Py+) NH ₂	cotton fabric	white light	<i>S. aureus</i>	9.5 J cm ⁻²	24 h
[122]	[5,10,15-tri(4- <i>N</i> -methylpyridyl)-20-(4-alkylphenyl)porphyrinato]zinc(II)	cotton fabric	white light	<i>S. aureus</i> <i>E. coli</i>	1000 lux	24 h
[123]	PPIX	cellulose	four 150 W tungsten bulbs (visible light)	<i>S. aureus</i> <i>E. coli</i>	1.7 mW cm ⁻²	24 h
[124]	5,10,15-tri(4-methylphenyl)-20-(4- <i>N</i> -methylpyridyl)porphyrin	cellulose	four 150 W tungsten bulbs (visible light)	<i>S. aureus</i> <i>E. coli</i>	1.7 mW cm ⁻²	24 h
[125]	5-[4-(3-carboxypropoxy)phenyl]-	cellulose	four 150 W tungsten bulbs	<i>S. aureus</i> <i>E. coli</i>	1.7 mW cm ⁻²	24 h

	10,15,20-tri(4-methylphenyl) porphyrin and 5-[4-(10-carboxydecanoxy)phenyl]-10,15,20-tri(4-methylphenyl) porphyrin		(visible light)			
[126]	[5,10,15-tri(4- <i>N</i> -methylpyridyl)-20-(4-alkylphenyl)porphyrinato]zinc(II)	CNC	white light (400–700 nm)	<i>E. coli</i> <i>S. aureus</i> <i>M. smegmatis</i>	54 J cm ⁻² 108 J cm ⁻²	15 min 30 min
[127]	[5,10,15-tri(4- <i>N</i> -methylpyridyl)-20-(4-alkylphenyl)porphyrinato]zinc(II)	CNC	visible light (400–700 nm)	<i>A. baumannii</i> <i>A. baumannii</i> (MDRAB) <i>S. aureus</i> (MRSA) <i>P. aeruginosa</i>	59 J cm ⁻² 118 J cm ⁻²	15 min 30 min
[128]	PPIX 5-(4-hydroxy phenyl)-10,15,20-tritoly porphyrin, 5-[4-(3-propargyloxy)phenyl]-10,15,20-tritoly porphyrin, [5-[4-(3-propargyloxy)phenyl]-10,15,20-tritoly porphyrinato]zinc(II)	cellulose	ten 23 W bulbs (visible light)	<i>E. coli</i> <i>S. aureus</i> <i>P. aeruginosa</i>	1.7 mW cm ⁻²	24 h
[129]	5-(4-aminophenyl)-10,15,20-tri(4- <i>N</i> -methylpyridyl)porphyrin	cellulose paper	LED model white Lambertian LXHL-MW1D 5500 K (white light)	<i>S. aureus</i> <i>E. coli</i>	9.5 J cm ⁻²	24 h
[135]	TPPN	polythiophene	white light	<i>E. coli</i> <i>B. subtilis</i>	90 mW cm ⁻²	5 min
[136]	5-(4-carboxyphenyl)-10,15,20-tris(4-methylphenyl)porphyrin	PDMS film	slide projector equipped with a 150 W lamp (350–800 nm)	<i>C. albicans</i>	90 mW cm ⁻²	60 min
[137]	5,10,15,20-tetra(4- <i>N,N</i> -diphenylaminophenyl)porphyrin and its Pd(II) complex	ITO films	Novamat 130 AF slide projector with a 150 W lamp (350–800 nm)	<i>E. coli</i> <i>C. albicans</i>	90 mW cm ⁻²	60 min
[138]	PPIX	MWNTs	compact fluorescence lamp 350 W, Sunlite (visible light)	<i>Influenza A virus</i>		5 min 10 min 15 min 30 min 45 min 60 min 90 min
[139]	PPIX	MWNTs	compact fluorescence lamp 350 W, Sunlite (visible light)	<i>S. aureus</i>		1 h
[147]	MnTPPS	porous honeycomb films immobilizer onto glass surface	100 W halogen bulb	<i>E. coli</i>		1 h
[148]	5,10,15-tri(<i>N</i> -methylpyridyl)-20-(<i>N</i> -tetradecylpyridyl) porphyrin	Silica microparticles	400 – 800 nm light	<i>E. coli</i> <i>S. aureus</i> (MRSA)	100 mW cm ⁻²	30 min
[149]	5-(2,3,4,5,6-pentafluorophenyl)-10,15,20-tripyridylporphyrin and the corresponding cationic 5,10,15-tri(4- <i>N</i> -methylpyridyl)-20-(2,3,4,5,6-pentafluorophenyl)porphyrins as tri-iodide salt	silica magnetic nanoparticles	13 parallel placed OSRAM lamps of 18 W each emitting in the 380e700 nm range	<i>A. fischeri</i>	40 W m ⁻²	24 h
[150]	5-(2,3,4,5,6-pentafluorophenyl)-10,15,20-tris(4-pyridyl)porphyrin, 5-(2,3,4,5,6-pentafluorophenyl)-10,15,20-tris(4- <i>N</i> -methylpyridyl) porphyrin tri iodide, 5-(2,3,4,5,6-	silica magnetic nanoparticles	13 parallel placed OSRAM lamps of 18 W each emitting in the 380e700 nm range	<i>E. coli</i> <i>E. faecalis</i>	40 W m ⁻²	90 min 180 min 270 min

	pentafluorophenyl)-10,15,20-triphenyl porphyrin					
[152]	TMePyP ⁴⁺	THES TMOS	white visible light	<i>E. coli</i>	7.9 J cm ⁻² 15.8 J cm ⁻²	1.5 h 3h
[153]	TPP ZnTPP	Electrospun PUR fibers	cold white light of a 150 W halogen bulb	<i>E. coli</i>		60 min
[154]	ClGaTCPP ClGaTCPP-PtNPs	PS	General electric Quartz line lamp (300 W) with a water filter	<i>S. aureus</i>	0.05 W cm ⁻²	30 min 60 min 90 min
[155]	TPP	Electrospun polystyrene nanofibers	400W solar simulator equipped with water filter	<i>E. coli</i>		5 min 10 min 15 min 20 min
[157]	TPP	PUR PS PCL PA-6	150 W halogen bulb (white light)	<i>E. coli</i>		5 min 10 min 15 min 20 min 25 min 30 min
[159]	PPIX ZnPP IX	Nylon fibers	Incandescent light	<i>E. coli</i> <i>S. aureus</i>	10000 lux 40000 lux 60000 lux	30 min
[160]	ANT DBTP	silica powder or beads	125 W lamp, emitting in the 200–600 nm range with UVA filter	<i>E. coli</i>	3.9 mW cm ⁻²	6 h
[163]	ER	CS	led source 540±5 nm	<i>S. mutans</i> <i>P. aeruginosa</i> <i>C. albicans</i>	25 J cm ⁻² 50 J cm ⁻²	
[164]	Cationic chlorin	3-bromopropyl- functionalized silica Merrifield resin	13 OSRAM lamps 18 W white light	<i>E. coli</i>	40 W m ²	3h

950

951 **Abbreviations**

ANT	9,10-anthraquinone 2-carboxylic acid
APTES	(3-aminopropyl) triethoxysilane
Bpac	4,4'-dicarboxy-2,2'-bipyridine
CDI	1,1'-carbonyldiimidazole
ClGaTCPP	[5,10,15,20-tetra-(4-carboxyphenyl) porphyrinato]gallium(III)chloride
ClGaTCPP-PtNPs	[5,10,15,20-tetra-(4-carboxyphenyl) porphyrinato]gallium(III)chloride conjugated with platinum nanoparticles
CNC	Nanocrystalline cellulose
CS	Chitosan
CSRB	Chitosan Rose Bengal conjugate
CMCPS	Chloromethylated crosslinked polystyrene microspheres
CSRBnp	Chitosan nanoparticles functionalized with Rose Bengal
CPS	Cross-linked polystyrene
DBTP	Benzo-[b]triphenylene-9,14-dicarbonitrile
DODMAB	Dimethyldioctadecyl-ammonium bromide
DMA	Dimethylacetamide
DPBF	1,2-diphenylisobenzofuran
DVB	Divinylbenzene
EDC	N-ethyl-N'-(3-dimethyl aminopropyl) carbodiimide

EMRSA	Epidemic strain of Methycillin Resistant <i>Staphylococcus aureus</i>
ER	Erythrosine
GlcNAc	1,4-linked N-acetyl-D-glucosamine
GlcN	D-glucosamine
Gram (+)	Gram positive
Gram (-)	Gram negative
HAI	Healthcare Associated Infections
HBA	Hydroxybenzaldehyde
ITO	Indium tin oxide
LBL	Layer by layer
LiCl	Lithium chloride
NHS	N-Hydroxysuccinimide
NMP	Nitroxide-mediated radical polymerization
MA	Maleic anhydride
MB	Methylene Blue
MES	2-(N-morpholino)ethanesulfonic acid
MDRAB	Multidrug-resistant <i>A. baumannii</i>
Min	Minutes
MnTPPS	[5,10,15,20-tetra(4-sodiumsulphonatophenyl)porphyrinato]manganese(III) chloride
MRSA	Methycillin Resistant <i>Staphylococcus aureus</i>
MWNTs	Multi-walled carbon nanotubes
¹ O ₂	Singlet oxygen
RB	Rose Bengal
RDP ²⁺	[tris(4,7-diphenyl-1,10-phenanthroline)-ruthenium(II)] dichloride
ROS	Reactive oxygen species
PACT	Photodynamic antimicrobial chemotherapy
PA-6	Polyamide 6
Pc	Phthalocyanine
PCL	Polycaprolactone
PDMS	Polydimethylsiloxane
PDMS-pAAc	Polydimethylsiloxane grafted acrylic acid
PMVE	Perfluorinated methyl vinyl ether
PbTpyPc	[2,9,16,23-tetra(4-pyridyloxy)phthalocyaninato]lead(II)
Pc	Phthalocyanine
PDMS	Polydimethylsiloxane
PDT	Photodynamic therapy
PEG	Polyethylene glycol
PMMA	Poly(methylmethacrylate)
PPIX	Protoporphyrin IX
Ps	Photosensitizer
PS	Polystyrene
PSil	Porous silicone
pXRD	Powder x-ray diffraction
PUR	Polyurethane
PVP	Poly(4-vinylpyridine)
p-THPP	5,10,15,20-tetra(4-hydroxyphenyl)porphyrin
p-TAPP	5,10,15,20-tetra(4-aminophenyl)porphyrin

PtNPs	Platinum nanoparticles
RNO	N,N-dimethyl-4-nitrosoaniline
TBO	Toluidine Blue O
TEOS	Tetraethylorthosilicate
TBZnPc	[2,9,16,23-tetra(4-terbutyl)phthalocyaninato]zinc(II)
THES	Tetrakis(2-hydroxyethoxy)silane
TMePyP ⁴⁺	5,10,15,20-tetra(4-N-methylpyridyl)porphyrin
TMOS	Tetramethoxysilane
TBZnPc	[2,9,16,23-tetra(4-terbutyl)phthalocyaninato]zinc(II)
TPP	5,10,15,20-tetraphenylporphyrin
TPP-NH ₂	5-(4-aminophenyl)-10,15,20-triphenylporphyrin
TPPN	5,10,15,20-tetra[4-(6-N,N,N-trimethylammoniumhexyloxy)phenyl]porphyrin bromide
TPPS-NH ₂	5-(4-aminophenyl)-10,15,20-tri(4-sulphonatophenyl)porphyrin
Trans(Me-Py ⁺) NH ₂	5-(4-methylpyridyl)-10,20-di(2,4,6-trimethylphenyl)-15-(4-aminophenyl)porphyrin
TSP	5,10,15,20-tetra(4-vinylphenyl)porphyrin
TTP	5,10,15,20-tetra(4-methylphenyl)porphyrin
ZnPcTs	(2,9,16,23-tetrasuphoxypthalocyaninato)zinc(II)
ZnPc	(phthalocyaninato)zinc(II)
ZnPcS	(2,9,16,23-tetrasuphoxypthalocyaninato)zinc(II) as tetrasodium salt
ZnTPP	(5,10,15,20-tetraphenylporphyrinato)zinc(II)

952

953

-
- [1] J.A. Al-Tawfiq, P.A. Tambyah, Healthcare associated infections (HAI) perspectives, *J. Infect. Public. Health.* 7 (2014) 339-344 doi: 10.1016/j.jiph.2014.04.003
- [2] S.E. Cosgrove, The Relationship between Antimicrobial Resistance and Patient Outcomes: Mortality, Length of Hospital Stay, and Health Care Costs, *Clin. Infect. Dis.* 42 (2006) S82-S89, doi: 10.1086/499406
- [3] Challenge, F. G. P. S. WHO Guidelines on Hand Hygiene in Health Care: a Summary. Geneva, Switzerland: World Health Organization, 2009, Available at: http://www.who.int/gpsc/5may/tools/who_guidelines-handhygiene_summary.pdf
- [4] G. Ducl, J. Fabry, L. Nicolle, Prevention of hospital-acquired infections: A practical guide, 2nd ed. Geneva, Switzerland: World Health Organization. Available at: <http://www.who.int/csr/resources/publications/whocdscsreph200212.pdf>
- [5] S.J. Dancer, The role of environmental cleaning in the control of hospital-acquired infection, *J. Hosp. Infect.* 73 (2009) 378-385 doi: 10.1016/j.jhin.2009.03.030
- [6] K. Page, M. Wilson, I. P. Parkin, Antimicrobial surfaces and their potential in reducing the role of the inanimate environment in the incidence of hospital-acquired infections, *J. Mater. Chem.* 19 (2009) 3819–3831 doi: 10.1039/b818698g
- [7] B. Allegranzi, S.B. Nejad, G.G. Castillejos, C. Kilpatrick, E. Kelley, Report on the Burden of Endemic Health Care–Associated Infection Worldwide. Geneva, Switzerland: World Health Organization. Available: http://whqlibdoc.who.int/publications/2011/9789241501507_eng.pdf
- [8] N. Ngwenya, E. Ncube, J. Parsons, Recent advances in drinking water disinfection: successes and challenges, in D.M. Whitacre (Eds), *Reviews of environmental contamination and toxicology*, Springer New York, 2013, pp. 111-170 doi:10.1007/978-1-4614-4717-7_4
- [9] X. Qu, J. Brame, Q. Li, P.J.J. Alvarez, Nanotechnology for a safe and sustainable water supply: enabling integrated water treatment and reuse, *Acc. Chem. Res.* 46 (2013) 834–843 doi: 10.1021/ar300029
- [10] D. Brown, J. Bridgeman, J.R. West, Predicting chlorine decay and THM formation in water supply systems, *Rev. Environ. Sci. Biotechnol.* 10 (2011) 79-99 doi:10.1007/s11157-011-9229-8
- [11] T.A. Ternes, J. Stüber, N. Herrmann, D. McDowell, A. Ried, M. Kampmann, B. Teiser, Ozonation: a tool for removal of pharmaceuticals, contrast media and musk fragrances from wastewater?, *Water Res.* 37 (2003) 1976-1982 doi: 10.1016/S0043-1354(02)00570-5
- [12] U. von Gunten, Ozonation of drinking water: part I. Oxidation kinetics and product formation, *Water Res.* 7 (2003) 1443-1467 doi:10.1016/S0043-1354(02)00457-8

-
- [13] U. von Gunten , Ozonation of drinking water: Part II. Disinfection and by-product formation in presence of bromide, iodide or chlorine, *Water Res.* 37 (2003) 1469-1487 doi:10.1016/S0043-1354(02)00458-X
- [14] W.W. Wu, M.M. Benjamin, G.V. Korshin, Effects of Thermal Treatment on Halogenated Disinfection By-Products in Drinking Water, *Wat. Res.* 35 (2001) 3545-3550 doi: 10.1016/S0043-1354(01)00080-X
- [15] W. Yang, H. Zhou, N. Cicek, Treatment of Organic Micropollutants in Water and Wastewater by UV-Based Processes: A Literature Review, *Crit. Rev. Env. Sci. Tec.* 44 (2014) 1443-1476 doi: 10.1080/10643389.2013.790745
- [16] M. Wainwright, In defence of 'dye therapy', *Int J Antimicrob Agents.* 44 (2014) 26-29. doi: 10.1016/j.ijantimicag.2014.02.013.
- [17] C.M. Cassidy, M.M. Tunney, P.A. McCarron, R.F. Donnelly, Drug delivery strategies for photodynamic antimicrobial chemotherapy: from benchtop to clinical practice. *J. Photochem. Photobiol. B.* 95 (2009) 71-80. doi: 10.1016/j.jphotobiol.2009.01.005
- [18] M. Wainwright, Photodynamic antimicrobial chemotherapy (PACT), *J. Antimicrob. Chemother.* 42 (1998) 13-28 doi: 10.1093/jac/42.1.13
- [19] T. Maisch, S. Hackbarth, J. Regensburger, A. Felgenträger, W. Bäumlner, M. Landthaler, B. Röder, Photodynamic inactivation of multi-resistant bacteria (PIB) – a new approach to treat superficial infections in the 21st century, *J. Dtsch. Dermatol. Ges.* 9 (2011) 360–366 doi: 10.1111/j.1610-0387.2010.07577.x
- [20] I.J. Macdonald, T.J. Dougherty, T. J. Basic principles of photodynamic therapy. *J. Porph. Phthal.* 5 (2002) 105–129. doi: 10.1002/jpp.328
- [21] M.C. DeRosa, R.J. Crutchley, Photosensitized singlet oxygen and its applications, *Coord. Chem. Rev.* 233-234 (2002) 351.- 371 doi: 10.1016/S0010-8545(02)00034-6
- [22] M.R. Hamblin, T. Hasan, Photodynamic therapy: a new antimicrobial approach to infectious disease?, *Photochem. Photobiol. Sci.* 3 (2004) 436–450 doi: 10.1039/B311900A
- [23] T. Maisch, A new strategy to destroy antibiotic resistant microorganisms: antimicrobial photodynamic treatment, *Mini Rev. Med. Chem.* 9 (2009) 974-983 doi: 10.2174/138955709788681582
- [24] A. Taraszkievicz, G. Fila, M. Grinholc, J. Nakonieczna, Innovative strategies to overcome biofilm resistance. *Biomed Res Int.* 2013 (2013) 150653 doi: 10.1155/2013/150653
- [25] D. Lazzeri, M. Rovera, L. Pascual, E.N. Durantini, Photodynamic studies and photoinactivation of *Escherichia coli* using meso-substituted cationic derivatives with asymmetric

charge distribution. *Photochem. Photobiol.* 80 (2) (2004) 286–293 doi: 10.1562/2004-03-08-RA-105.1

[26] S. Banfi, E. Caruso, L. Buccafurni, V. Battini, S. Zazzaron, P. Barbieri, V. Orlandi, Antibacterial activity of tetraaryl-porphyrin photosensitizers: an in vitro study on Gram negative and Gram positive bacteria, *J Photochem Photobiol B.* 85 (1) (2006) 28-38 doi: 10.1016/j.jphotobiol.2006.04.003

[27] F.F. Sperandio, Y.Y. Huang and, M.R. Hamblin, Antimicrobial Photodynamic Therapy to Kill Gram-negative Bacteria, *Recent. Pat. Antiinfect. Drug. Discov.* 8 (2) 108-120 doi: 10.2174/1574891X113089990012

[28] J.P. Rolim, M.A. de-Melo, S.F. Guedes, F.B. Albuquerque-Filho, J.R. de Souza, N.A. Nogueira, I.C. Zanin, L.K. Rodrigues, The antimicrobial activity of photodynamic therapy against *Streptococcus mutans* using different photosensitizers, *J Photochem Photobiol B.* 106 (2012) 40-46 doi: 10.1016/j.jphotobiol.2011.10.001

[29] N. Komerik, H. Nakanishi, A.J. MacRobert, B. Henderson, P. Speight, M. Wilson, In Vivo Killing of *Porphyromonas gingivalis* by Toluidine Blue-Mediated Photosensitization in an Animal Model, *Antimicrob. Agents Chemother.* 47 (3) (2003) 932–940 doi: 10.1128/AAC.47.3.932-940.2003

[30] C.F. Lee, C.J. Lee, C.T. Chen, C.T. Huang, δ -Aminolaevulinic acid mediated photodynamic antimicrobial chemotherapy on *Pseudomonas aeruginosa* planktonic and biofilm cultures, *J. Photochem. Photobiol. B* 75 (2004) 21–25 doi: 10.1016/j.jphotobiol.2004.04.003

[31] G. Jori, M. Camerin, M. Soncin, L. Guidolin, O. Coppellotti, Antimicrobial Photodynamic Therapy: Basic Principles, in M.R Hamblin (Eds), G. Jori (Eds), *Photodynamic Inactivation of Microbial Pathogens. Medical and Environmental Applications*, The Royal Society of Chemistry, Cambridge, UK, 2011 pp. 1-18 doi: 10.1039/9781849733083-00001

[32] T. Maisch, R.M. Szeimies, G. Jori, C. Abels, Antibacterial photodynamic therapy in dermatology, *Photochem. Photobiol. Sci.* 3 (2004) 907-917 doi: 10.1039/B407622B

[33] H. Nikaido, Prevention of drug access to bacterial targets: Permeability barrier and active efflux, *Science* 264 (1994) 362–368 doi:10.1126/science.8153625

[34] Z. Malik, H. Ladan, Y. Nitzan, Photodynamic inactivation of Gram-negative bacteria: problems and possible solutions. *J. Photochem. Photobiol. B.* 14 (1992) 262–266 doi: 10.1016/1011-1344(92)85104-3

-
- [35] K. O’Riordan, O. E. Akilov, T. Hasan, The potential for photodynamic therapy in the treatment of localized infections, *Photodiagnosis Photodyn Ther.* 2 (2005) 247–262 doi: 10.1016/S1572-1000(05)00099-2
- [36] M. Jemli, Z. Alouini, S. Sabbahi, M. Gueddari, Destruction of fecal bacteria in wastewater by three photosensitizers, *J. Environ. Monit.* 4 (2002) 511-516 doi: 10.1039/b204637g
- [37] M. Wainwright, *Photosensitizers in biomedicine*, first ed., Wiley Blackwell, West Sussex, 2009 ISBN: 978-0-470-51060-5
- [38] M. Wainwright, Non-porphyrin photosensitizers in biomedicine, *Chem. Soc. Rev.* 25 (1996) 351-359 doi: 10.1039/CS9962500351
- [39] A. Ramos, T.M. Braga, S.S. Braga, Ru(II)-based antimicrobials: looking beyond organic drugs, *Mini Rev. Med. Chem.* 12 (2012) 227-235 doi: 10.2174/1389557511209030227
- [40] A. Almeida, A. Cunha, M.A.F. Faustino, A.C. Tomé, M.G.P.M.S. Neves, Porphyrins as Antimicrobial Photosensitizing Agents, in M.R Hamblin (Eds), G. Jori (Eds), *Photodynamic Inactivation of Microbial Pathogens. Medical and Environmental Applications*, The Royal Society of Chemistry, Cambridge, UK, 2011 pp. 83-160 doi: 10.1039/9781849733083-00083
- [41] T.A. Dahl, W.R. Middenand, P.E. Hartman, Pure singlet oxygen cytotoxicity for bacteria, *Photochem. Photobiol.* 46 (1987) 345–352 doi: 10.1111/j.1751-1097.1987.tb04779.x
- [42] R. Cahan, Conjugated and immobilized photosensitizers for combating bacterial infections, *Recent Pat. Antiinfect. Drug Discov.* 8 (2013) 121-129 doi: 10.2174/1574891X113089990010
- [43] M. Wainwright, The development of phenothiazinium photosensitisers, *Photodiagnosis Photodyn Ther.* 4 (2005) 263-272. doi: 10.1016/S1572-1000(05)00110-9.
- [44] F. Harris, L.K. Chatfield, D.A. Phoenix, Phenothiazinium Based Photosensitisers - Photodynamic Agents with a Multiplicity of Cellular Targets and Clinical Applications, *Curr. Drug Targets* 6 (2005) 615-627 doi: 10.2174/1389450054545962
- [45] J.P. Tardivo, A. Del Giglio, C. Santos de Oliveira, D.S. Gabrielli, H.C. Junqueira, D.B. Tada, D. Severino, R.F. Turchiello, M.S. Baptista, Methylene blue in photodynamic therapy: From basic mechanisms to clinical applications, *Photodiagnosis Photodyn Ther.* 2 (2005) 175-191 doi:10.1016/S1572-1000(05)00097-9
- [46] M. Wainwright, Methylene blue derivatives — suitable photoantimicrobials for blood product disinfection? *Int. J. Antimicrob. Ag.* 16 (2000) 381-394 doi: [http://dx.doi.org/10.1016/S0924-8579\(00\)00207-7](http://dx.doi.org/10.1016/S0924-8579(00)00207-7)

-
- [47] S. Perni, P. Prokopovich, I.P. Parkin, M. Wilson, J. Pratten, Prevention of biofilm accumulation on a light-activated antimicrobial catheter material, *J. Mater. Chem.* 20 (2010) 8668–8673 doi: 10.1039/c0jm01891k
- [48] S. Perni, C. Piccirillo; A. Kafizas; M. Uppal; J. Pratten, M. Wilson, I.P. Parkin, Antibacterial Activity of Light-Activated Silicone Containing Methylene Blue and Gold Nanoparticles of Different Sizes, *J. Clust. Sci.* 21 (2010) 427 – 438 doi: 10.1007/s10876-010-0319-5
- [49] C. Piccirillo , S. Perni , J. Gil-Thomas , P. Prokopovich , M. Wilson , J. Pratten , I.P. Parkin , Antimicrobial activity of methylene blue and toluidine blue O covalently bound to a modified silicone polymer surface, *J. Mater. Chem.* 19 (2009) 6167–6171 doi: 10.1039/b905495b
- [50] S. Ismail, S. Perni, J. Pratten, I. Parkin, M. Wilson, Efficacy of a novel light-activated antimicrobial coating for disinfecting hospital surfaces, *Infect. Control Hosp. Epidemiol.* 32 (2011) 1130-1132 doi: 10.1086/662377
- [51] A.J.T. Naik, S. Ismail, C. Kay, M. Wilson, I.P. Parkin, Antimicrobial activity of polyurethane embedded with methylene blue, toluidene blue and gold nanoparticles against *Staphylococcus aureus*; illuminated with white light, *Mater. Chem. Phys.* 129 (2011) 446–450 doi:10.1016/j.matchemphys.2011.04.040
- [52] S. Perni, P. Prokopovich, C. Piccirillo, J.R. Pratten, I.P. Parkin, M. Wilson. Toluidine Blue-Containing Polymers exhibit Bactericidal Activity When Irradiated with Red Light, *J. Mater. Chem.* 19 (2009) 2715–2723 doi: 10.1039/b820561b
- [53] R. Cahan, R. Schwartz, Y. Langzam, Y. Nitzan, Light-activated antibacterial surfaces comprise photosensitizers, *Photochem Photobiol.* 87 (2011) 1379-1386 doi: 10.1111/j.1751-1097.2011.00989.x
- [54] M. Wilson, Light activated antimicrobial coating for the continuous disinfection of surfaces, *Infect. Control Hosp. Epidemiol.* 24 (2003) 782–784 doi: 10.1086/502136
- [55] V. Decraene, J. Pratten, M. Wilson, Cellulose acetate containing toluidine blue and rose bengal is an effective antimicrobial coating when exposed to white light, *Appl. Environ. Microbiol.* 72 (2006) 4436–4439 doi:10.1128/AEM.02945-05
- [56] V. Decraene, J. Pratten, M. Wilson, Novel light-activated antimicrobial coatings are effective against surface-deposited *Staphylococcus aureus*, *Curr. Microbiol.* 57 (2008) 269–273 doi: 10.1007/s00284-008-9188-7
- [57] S. Perni, C. Piccirillo, J. Pratten, P. Prokopovich, W. Chrzanowski, I.P. Parkin, M. Wilson, The antimicrobial properties of light-activated polymers containing methylene blue and gold nanoparticles, *Biomaterials* 30 (2009) 89–93 doi:10.1016/j.biomaterials.2008.09.020

-
- [58] A. Simmons, J. Hyvarinen, L. Poole-Warren, The effect of sterilisation on a poly(dimethylsiloxane)/poly(hexamethylene oxide) mixed macrodiol-based polyurethane elastomer, *Biomaterials* 27 (2006) 4484–4497 doi:10.1016/j.biomaterials.2006.04.017
- [59] K. Gorna, S. Gogolewski, Molecular stability, mechanical properties, surface characteristics and sterility of biodegradable polyurethanes treated with low-temperature plasma, *Pol. Degrad. Stabil.* 79 (2003) 475–485 doi: 10.1016/S0141-3910(02)00363-4
- [60] T. Tsai, H.-F. Chien, T.-H. Wang, C.-T. Huang, Y.-B. Ker, C.-T. Chen, Chitosan augments photodynamic inactivation of gram-positive and gram-negative bacteria, *Antimicrob. Agents Chemother.* 55 (2011) 1883-1890. doi:10.1128/AAC.00550-10
- [61] R.F. Donnelly, P.A. McCarron, M.M. Tunney, A.D. Woolfson, Potential of photodynamic therapy in treatment of fungal infections of the mouth. Design and characterisation of a mucoadhesive patch containing toluidine blue O, *J. Photochem. Photobiol. B* 86 (2007) 59-69 doi:10.1016/j.jphotobiol.2006.07.011
- [62] M. Wainwright, M.N. Byrne, M.A. Gattrell, Phenothiazinium-based photobactericidal materials, *J. Photochem. Photobiol. B* 84 (2006) 227-230 doi:10.1016/j.jphotobiol.2006.03.002
- [63] J. Gil-Tomas, S. Tubby, I.P. Parkin, N. Narband, L. Dekker, S.P. Nair, M. Wilson, C. Street, Lethal photosensitisation of *Staphylococcus aureus* using a toluidine blue O-tiopronin-gold nanoparticle conjugate, *J. Mater. Chem.* 17 (2007) 3739–3746 doi: 10.1039/b706615e
- [64] A. Savino A., G. Angeli, Phoyodynamic inactivation of e. coli by immobilized or coated dyes on insoluble supports, *Water Res.* 19 (1985) 1465-1469 doi: 10.1016/0043-1354(85)90390-2
- [65] P.A. Suci, Z. Varpness, E. Gillitzer, T. Douglas, M. Young, Targeting and Photodynamic Killing of a Microbial Pathogen Using Protein Cage Architectures Functionalized with a Photosensitizer, *Langmuir* 23 (2007) 12280 – 12286 doi: 10.1021/la7021424
- [66] G. Subramanian, P. Parakh, H. Prakash, Photodegradation of methyl orange and photoinactivation of bacteria by visible light activation of persulphate using a tris (2,2'-bipyridyl)ruthenium(II) complex, *Photochem. Photobiol. Sci.* 12 (2013) 456-466 doi: 10.1039/c2pp25316j
- [67] P. Parakh, S. Gokulakrishnan, H. Prakash, Visible light water disinfection using [Ru(bpy)₂(phendione)](PF₆)₂·2H₂O and [Ru(phendione)₃]Cl₂·2H₂O complexes and their effective adsorption onto activated carbon, *Sep. Purific. Technol.* 109 (2013) 9–17 doi: <http://dx.doi.org/10.1016/j.seppur.2013.02.022>
- [68] W. Lei, Q. Zhou, G. Jiang, B. Zhang, X. Wang, Photodynamic inactivation of *Escherichia coli* by Ru(II) complexes, *Photochem. Photobiol. Sci.* 10 (2011) 887-890 doi: 10.1039/c0pp00275e

-
- [69] Y. Liu, R. Hammitt, D.A. Lutterman, L.E. Joyce, R.P. Thummel, C. Turro, Ru(II) complexes of new tridentate ligands: unexpected high yield of sensitized $^1\text{O}_2$, *Inorg. Chem.* 48 (2009) 375-385 doi: 10.1021/ic801636u
- [70] A.A. Abdel-Shafi, D.R. Worrall, A.Y. Ershov, Photosensitized generation of singlet oxygen from ruthenium(II) and osmium(II) bipyridyl complexes, *Dalton Trans.* 7 (2004) 30-36 doi: 10.1039/b310238f
- [71] J.L. Bourdelande, J. Font, G. Marques, A.A. Abdel-Shafi, F. Wilkinson, D.R. Worrall, On the efficiency of the photosensitized production of singlet oxygen in water suspensions of a tris(bipyridyl)ruthenium(II) complex covalently bound to an insoluble hydrophilic polymer, *J. Photochem. Photobiol. A* 138 (2001) 65-68 doi: 10.1016/S1010-6030(00)00385-3
- [72] M.E. Jimenez-Hernandez, F. Manjon, D. Garcia-Fresnadillo, G. Orellana, Solar water disinfection by singlet oxygen photogenerated with polymer-supported Ru(II) sensitizers, *Solar Energy* 80 (2006) 1382-1387 doi:10.1016/j.solener.2005.04.027
- [73] F. Manjón, M. Santana-Magaña, D. García-Fresnadillo, G. Orellana G. Are silicone-supported [C60]-fullerenes an alternative to Ru(II) polypyridyls for photodynamic solar water disinfection?, *Photochem Photobiol Sci.* 13 (2014) 397-406 doi: 10.1039/c3pp50361e
- [74] F. Manjón, D. García-Fresnadillo, G. Orellana, Water disinfection with Ru(II) photosensitisers supported on ionic porous silicones, *Photochem Photobiol Sci.* 8 (2009) 926-932 doi: 10.1039/b902014d
- [75] F. Manjón, M. Santana-Magaña, D. García-Fresnadillo, G. Orellana, Singlet oxygen sensitizing materials based on porous silicone: Photochemical characterization, effect of dye reloading and application to water disinfection with solar reactors, *Photochem. Photobiol. Sci.* 9 (2010) 838-845 doi: 10.1039/c0pp00026d
- [76] L. Villén, F. Manjón, D. García-Fresnadillo, G. Orellana, Solar water disinfection by photocatalytic singlet oxygen production in heterogeneous medium, *Applied Catalysis B: Environmental* 69 (2006) 1-9 doi: 10.1016/j.apcatb.2006.05.015
- [77] T.A. Dahl, W.R. Midden, D.C. Neckers, Comparison of photodynamic action by Rose Bengal in gram-positive and gram-negative bacteria, *Photochem. Photobiol.* 48 (1988) 607-612 doi: 10.1111/j.1751-1097.1988.tb02870.x
- [78] K. Ergaieg, R. Seux, A comparative study of the photoinactivation of bacteria by meso-substituted cationic porphyrin, rose Bengal and methylene blue, *Desalination* 246 (2009) 353-362 doi: 10.1016/j.desal.2008.03.060

-
- [79] M. Schafer, C. Schmitz, R. Facius, G. Horneck, B. Milow, K. H. Funken, J. Ortner, Systematic Study of Parameters Influencing the Action of Rose Bengal with Visible Light on Bacterial Cells: Comparison Between the Biological Effect and Singlet-Oxygen Production, *Photochem. Photobiol.* 71 (2000) 514–523 doi: [http://dx.doi.org/10.1562/0031-8655\(2000\)071<0514:SSOPIT>2.0.CO;2](http://dx.doi.org/10.1562/0031-8655(2000)071<0514:SSOPIT>2.0.CO;2)
- [80] L. Moczek and M. Nowakowska, Novel water-soluble photosensitisers from chitosan, *Biomacromolecules* 8 (2007) 433–438 doi: 10.1021/bm060454
- [81] A. Shrestha, M.R. Hamblin, A. Kishen, Photoactivated Rose Bengal functionalised chitosan nanoparticles produce antibacterial/biofilm activity and stabilise dentin-collagen, *Nanomed. Nanotech. Biol. Med.* 10 (2014) 491-501 doi: 10.1016/j.nano.2013.10.010
- [82] A. Shrestha, A. Kishen, Antibacterial Efficacy of Photosensitizer Functionalized Biopolymeric Nanoparticles in the Presence of Tissue Inhibitors, Root Canal, *J. Endodont.* 40 (2014) 566–570 doi: <http://dx.doi.org/10.1016/j.joen.2013.09.013>
- [83] A.M. Ferreira, I. Carmagnola, V. Chiono, P. Gentile, L. Fracchia, C. Ceresa, G. Georgiev, G. Ciardelli, Surface modification of poly(dimethylsiloxane) by two-step plasma treatment for further grafting with chitosan-Rose Bengal photosensitizer, *Surf. Coatings Technol.* 223 (2013) 92–97 doi: 10.1016/l.surfcoat.2013.02.035
- [84] A. Shrestha, A. Kishen, Polycationic chitosan-conjugated photosensitizer for antibacterial photodynamic therapy, *Photochem. Photobiol.* 88 (2012) 577-583 doi: 10.1111/j.1751-1097.2011.01026.x
- [85] A. Shrestha, M.R. Hamblin, A. Kishen, Characterization of a conjugate between Rose Bengal and chitosan for targeted antibiofilm and tissue stabilization effects as a potential treatment of infected dentin, *Antimicrob. Agents. Chemother.* 56 (2012) 4876–4884 doi: 10.1128/AAC.00810-12
- [86] E.I. Rabea, M.E. Badawy, C.V. Stevens, G. Smagghe, W. Steurbaut, Chitosan as antimicrobial agent: applications and mode of action, *Biomacromolecules* 4 (2003) 1457–1465 doi: 10.1021/bm034130m
- [87] M. Kong, X.G. Chen, K. Xing, H.J. Park, Antimicrobial properties of chitosan and mode of action: a state of the art review, *Int. J. Food Microbiol.* 144 (2010) 51-63 doi: 10.1016/j.ijfoodmicro.2010.09.012
- [88] M.Z. Elsabee, E.S. Abdoub, Chitosan based edible films and coatings: A review, *Mat. Sci. Eng. C* 33 (2013) 1819–1841 doi:10.1016/j.msec.2013.01.010
- [89] A. Jimtaisong, N. Saewan, Utilization of carboxymethyl chitosan in cosmetics. *Int. J. Cosmetic Sci.* 36 (2014) 12–21 doi:10.1111/ics.12102

-
- [90] P. Laurienzo, Marine polysaccharides in pharmaceutical applications: An overview, *Mar. Drugs* 8 (2010) 2435-2465 doi:10.3390/md8092435
- [91] C. Xu, C. Lei, L. Meng, C. Wang, Y. Song, Chitosan as a barrier membrane material in periodontal tissue regeneration, *J. Biomed. Mater. Res. Part B* 100B (2012) 1435–1443 doi: 10.1002/jbm.b.32662
- [92] Y. Guo, S. Rogelj, P. Zhang, Rose Bengal- decorated silica nanoparticles as photosensitisers for inactivation of gram- positive bacteria, *Nanotechnology* 21 (2010) 065102-065109 doi: 10.1088/0957-4484/21/6/065102
- [93] L. Pessoni, S. Lacombe, L. Billon, R. Brown, M. Save, Photoactive, Porous Honeycomb Films Prepared from Rose Bengal-Grafted Polystyrene, *Langmuir* 29 (2013) 10264–10271 doi: 10.1021/la402079z
- [94] F. Nakonechny, A. Pinkus, S. Hai, O. Yehosha, Y. Nitzan, M. Nisnevitch, Eradication of Gram-positive and Gram-negative bacteria by photosensitizers immobilized in polystyrene. *Photochem. Photobiol.* 89 (2013) 671–678 doi: 10.1111/php.12022
- [95] J. Johson Inbaraj, M.V. Vinodu, R. Gandhidasan, R. Murugesan, M. Padmanabhan, Photosensitizing properties of ionic porphyrins immobilized on functionalized solid polystyrene support, *J. Appl. Polym. Sci.* 89 (2003) 3925-3930 doi: 10.1002/app.12610
- [96] S.A Bezman, P.A. Burtis, T.P.J. Izod, M.A. Thayer, Photodynamic inactivation of *E. coli* by rose bengal immobilized on polystyrene beads, *Photochem. Photobiol.* 28 (1978) 325-329 doi: 10.1111/j.1751-1097.1978.tb07714.x
- [97] M. Nowakowska, M. Kepczyński, K. Szczubialka, Polymeric photosensitizers, 1. Synthesis and photochemical properties of poly[(sodium *p*-styrenesulfonate)-*co*-(4-vinylbenzyl chloride)] containing rose bengal chromophores, *Macromol. Chem. Phys.* 196 (1995) 2073–2080. doi: 10.1002/macp.1995.021960626
- [98] M. Nowakowska, M. Kepcynski, Polymeric photosensitizers 2. Photosensitized oxidation of phenol in aqueous solution, *J. Photochem. Photobiol. A: Chem.* 116 (1998) 251-256 doi: 10.1016/S1010-6030(98)00305-0
- [99] A.P. Schaap, A.L. Thayer, E.C. Blossey, D.C. Neckers., Polymer-based sensitizers for photooxidations II, *J. Am. Chem. Soc.* 97 (1975) 3741–3745 doi: 10.1021/ja00846a030
- [100] A. Minnock, D.I. Vernon, J. Schofield, J. Griffiths, J.H. Parish, S.B. Brown, Photoinactivation of bacteria. Use of a cationic water-soluble zinc phthalocyanine to photoinactivate both Gram-negative and Gram-positive bacteria, *J. Photochem. Photobiol. B* 32 (1996) 159-164 doi: 10.1016/1011-1344(95)07148-2

-
- [101] V. Mantareva, V. Kussovski, I. Angelov, E. Borisova, L. Avramov, G. Schnurpfeil, D. Wöhrle, Photodynamic activity of water-soluble phthalocyanine zinc(II) complexes against pathogenic microorganisms, *Bioorg. Med. Chem.* 15 (2007) 4829-4835 doi:10.1016/j.bmc.2007.04.069
- [102] V. Mantareva, V. Kussovski, I. Angelov, D. Wöhrle, R. Dimitrov, E. Popova, S. Dimitrov, Non-aggregated Ga(III)-phthalocyanines in the photodynamic inactivation of planktonic and biofilm cultures of pathogenic microorganisms. *Photochem. Photobiol. Sci.* 10 (2011) 91-102 doi: 10.1039/b9pp00154a
- [103] R.F. Donnelly, P.A. McCarron, M.M. Tunney, Antifungal photodynamic therapy, *Microbiol. Res.* 163 (2008) 1–12 doi: 10.1016/j.micres.2007.08.001
- [104] J. Chen, Z. Chen, Y. Zheng, S. Zhou, J. Wang, N. Chen, J. Huang, F. Yan, M. Huang, Substituted zinc phthalocyanine as an antimicrobial photosensitizer for periodontitis treatment, *J Porph Phthaloc* 15 (2011) 293-299 doi: 10.1142/S1088424611003276
- [105] O.L. Osifeko, T. Nyokong, Applications of lead phthalocyanines embedded in electrospun fibers for the photoinactivation of *Escherichia coli* in water, *Dye Pigments* 111 (2014) 8–15, doi: 10.1016/j.dyepig.2014.05.010
- [106] N. Masilela, P. Kleyi, Z. Tshentu, G. Priniotakis, P. Westbroek, T. Nyokong, Photodynamic inactivation of *Staphylococcus aureus* using low symmetrically substituted phthalocyanines supported on a polystyrene polymer fiber, *Dye Pigments* 96 (2013) 500–508 doi: 10.1016/j.dyepig.2012.10.001
- [107] S. Tombe, E. Antunes, T. Nyokong, Electrospun fibers functionalized with phthalocyanine-gold nanoparticle conjugates for photocatalytic applications, *J. Mol. Catal. A: Chem.* 371 (2013) 125–134 doi: 10.1016/j.molcata.2013.01.033
- [108] J. Mosinger, K. Lang, P. Kubát, J. Sýkora, M. Hof, L. Plístil, and B. Mosinger, Photofunctional polyurethane nanofabrics doped by zinc tetraphenyl porphyrin and zinc phthalocyanine photosensitisers, *J. Fluoresc.* 19 (2009) 705–713 doi: 10.1007/s10895-009-0464-0
- [109] S. Tang, C. Shao, Y. Liu, S. Li, R. Mu, Electrospun nanofibers of poly(ethyleneoxide)/tetraaminophthalocyanine copper (II) hybrids and its photoluminescence properties, *J. Phys. Chem. Solids* 68 (2007) 2337-2340 doi:10.1016/j.jpcs.2007.07.014
- [110] Z.M Huang, Y.-Z. Zhang, M. Kotaki, S. Ramakrishna, A review on polymer nanofibers by electrospinning and their applications in nanocomposites, *Comp. Sci. Technol.* 63 (2003) 2223–2253 doi:10.1016/S0266-3538(03)00178-7

-
- [111] P. Modisha, T. Nyokong, Fabrication of phthalocyanine-magnetic nanoparticles hybrid nanofibers for degradation of Orange-G, *J. Mol. Catal. A: Chem.* 381 (2014) 132-137 doi: 10.1016/j.molcata.2013.10.012
- [112] A. Goethals, T. Mugadza, Y. Arslanoglu, R. Zugle, E. Antunes, S.W.H. Van Hulle, T. Nyokong, K. De Clerck, Polyamide nanofiber membranes functionalized with zinc phthalocyanines, *J. Appl. Polym. Sci.* 131 (2014) 40486-40473 doi: 10.1002/app.40486
- [113] S. Artarsky, S. Dimitrova, R. Bonnett, M. Krysteva, Immobilisation of Zinc Phthalocyanines in silicate matrices and investigation of their photobactericidal effect on *E. coli*, *TheScientificWorld Journal* 6 (2006) 374–382 doi: 10.1100/tsb.2006.75.
- [114] R. Bonnett, D.G. Buckley, T. Burrow, A.B.B. Galia, B. Savilleb, S.P. Songca, Photobactericidal materials based on Porphyrins and Phthalocyanines, *J. Mater. Chem.* 3 (1993) 323–324 doi: 10.1039/JM9930300323
- [115] R. Bonnett, M. A. Krysteva, I. G. Lalov, S. V. Artarsky, Water disinfection using photosensitisers immobilised on chitosan, *Water Res.* 40 (2006) 1269–1275 doi: 10.1016/j.watres.2006.01.014
- [116] K. Sakakibara, F. Nakatsubo, A. D. French, T. Rosenau, Chiroptical properties of an alternately functionalised cellotriose bearing two porphyrin groups, *Chem. Commun.* 48 (2012) 7672–7674 doi: 10.1039/c2cc30805c
- [117] V.S. Gaware, M. Håkerud, K. Leósson, S. Jónsdóttir, A. Høgset, K. Berg, M. Másson, Tetraphenylporphyrin tethered chitosan based carriers for photochemical transfection, *J. Med. Chem.* 56 (2013) 807–819 doi: 10.1021/jm301270r
- [118] R. Lucas, R. Granet, V. Sol, C. Le Morvan, E. Rivière, P. Krausz, L. De Chimie, A. Albert, Synthesis and cellular uptake of superparamagnetic dextran-nanoparticles with porphyrinic motifs grafted by esterification, *E-polymers* 089 (2007) 1031–1038 doi: 10.1515/epoly.2007.7.1.1031
- [119] H. Jiang, W. Su, J. Hazel, J. T. Grant, V.mV. Tsukruk, T. M. Cooper, T. J. Bunning, Electrostatic self-assembly of sulfonated C60 – porphyrin complexes on chitosan thin films, *Thin solid films* 372 (2000) 85-93 doi: 10.1016/S0040-6090(00)01033-6
- [120] C. Ringot, V. Sol, M. Barriere, N. Saad, P. Bressollier, R. Granet, P. Couleaud, C.Frochot, P. Krausz, Triazinyl Porphyrin- based photoactive cotton fabrics: preparation, characterization and antibacterial activity, *Biomacromolecules* 12 (2011) 1716-1723, doi: 10.1021/bm200082d
- [121] C. Ringot, N. Saad, R. Granet, P. Bressollier, V. Sol, P. Krausz, Meso-functionalized aminoporphyrins as efficient agents for photo-bactericidal surfaces, *J. Porphyrins Phthalocyanines* 14 (2010) 925–931 doi: 10.1142/S1088424610002719

-
- [122] C. Ringot, V. Sol, R. Granet, P. Krausz, Porphyrin-grafted cellulose fabric: New photobactericidal material obtained by “click-chemistry” reaction, *Mat. Let.* 63 (2009) 1889-1891, doi: 10.1016/j.matlet.2009.06.009
- [123] M. Krouit, R. Granet, P. Branland, B. Verneuil, P. Krausz, New photoantimicrobial films composed of porphyrinated lipophilic cellulose esters, *Bioorg. Med. Chem. Lett.* 16 (2006) 1651–1655 doi: 10.1016/j.bmcl.2005.12.008
- [124] M. Krouit, R. Granet, P. Krausz, Photobactericidal plastic films based on cellulose esterified by chloroacetate and a cationic porphyrin, *Bioorgan. Med. Chem.* 16 (2008) 10091- 10097 doi: 10.1016/j.bmc.2008.10.010
- [125] M. Krouit, R. Granet, P. Krausz, Photobactericidal films from porphyrins grafted to alkylated cellulose – synthesis and bactericidal properties, *Eur. Polym. J.* 45 (2009) 1250-1259, doi: 10.1016/j.eurpolymj.2008.11.036
- [126] E. Feese, H. Sadeghifar, H.S.Gracz, D.S. Argyropoulos, R.A. Ghiladi, Photobactericidal porphyrin-cellulose nanocrystals: synthesis, characterisation and antimicrobial properties, *Biomacromolecules* 12 (2011) 3528- 3539 doi: 10.1021/bm200718s
- [127] B.L. Carpenter, E. Feese, H. Sadeghifar, D.S. Argyropoulos, R.A. Ghiladi, Porphyrin-cellulose nanocrystals: a photobactericidal material that exhibits broad spectrum antimicrobial activity. *Photochem. Photobiol.* 88 (2012) 527-536. doi: 10.1111/j.1751-1097.2012.01117.x
- [128] A. Memmi, R. Granet, M. Aouni, A. Bakhrouf, P. Krausz, Synthesis of new photobactericidal polymers by “click chemistry” and a study of their biological activity, *e-Polymers* 12 (2012) 467–478 doi: 10.1515/epoly.2012.12.1.467
- [129] J.P. Mbakidi, K. Herke, S. Alves, V. Chaleix, R. Granet, P. Krausz, S. Leroy-Lhez, T.S. Ouk, V. Sol, Synthesis and photobiocidal properties of cationic porphyrin-grafted paper, *Carbohydr. Polym.* 91 (2013) 333-338 doi: 10.1016/j.carbpol.2012.08.013
- [130] M. Mukherjee, A.R. Ray, Biomimetic oxidation of L-arginine with hydrogen peroxide catalysed by the resin-supported iron (III) porphyrin, *J. Mol. Cat. A-Chem.* 266 (2007) 207-214 doi: 10.1016/j.molcata.2006.11.012
- [131] E. Brule, Y.R. deMiguel, K. Kuok, Chemoselective epoxidation of dienes using polymer-supported manganese porphyrin catalysts, *Tetrahedron* 60 (2004) 5913-5918 doi: 10.1016/j.tet.2004.05.026
- [132] S.M. Ribeiro, A.C. Serra, A.M. d’A. Rocha Gonsalves, Covalently immobilised porphyrins as photooxidation catalysts, *Tetrahedron* 63 (2007) 7885-7891 doi: 10.1016/j.tet.2007.05.084

-
- [133] V. Vasil'ev, S. M. Borisov, Optical oxygen sensors based on phosphorescent water-soluble platinum metal porphyrins immobilised in perfluorinated ion-exchange membrane, *Sens. Actuat. B-Chem* 82 (2002) 272-276 doi: 10.1016/S0925-4005(01)01063-2
- [134] D. Faust, K.-H. Funken, G. Horneck, B. Milow, J. Ortner, M. Sattlegger, M. Schäfer, C. Schmitz, Immobilized Photosensitizers for solar photochemical applications, *Solar Energy* 65 (1999) 71–74 doi: 10.1016/S0038-092X(98)00099-1
- [135] C.F. Xing, Q.L. Xu, H.W. Tang, L.B. Liu, S. Wang, Conjugated polymer/porphyrin complexes for efficient energy transfer and improving light-activated antibacterial activity, *J. Am. Chem. Soc.* 131 (2009) 13117–13124 doi: 10.1021/ja904492x
- [136] M.G. Alvarez, M.L. Gómez, S.J. Mora, M.E. Milanesio, E.N. Durantini, Photodynamic inactivation of *Candida albicans* using bridged polysilsesquioxane films doped with porphyrin *Bioorg. Med. Chem.* 20 (2012) 4032-4039 doi: 10.1016/j.bmc.2012.05.012
- [137] M.D. Funes, D.A. Caminos, M.G. Alvarez, F. Fungo, L.A. Otero, E.N. Durantini, Photodynamic properties and photoantimicrobial action of electrochemically generated porphyrin polymeric films, *Environ. Sci. Technol.* 43 (2009) 902-908 doi: 10.1021/es802450b
- [138] I. Banerjee, M.P. Douaisi, D. Mondal, R.S. Kane, Light-activated nanotube-porphyrin conjugates as effective antiviral agents, *Nanotechnology* 23 (2012) 105101- 105107 doi: 10.1088/0957-4484/23/10/105101
- [139] I. Banerjee, D. Mondal, J. Martin, R.S. Kane, Photoactivated Antimicrobial Activity of Carbon Nanotube - Porphyrin Conjugates, *Langmuir*, 26 (2010) 17369-17374 doi: 10.1021/1103298e
- [140] B. Gao, L. Fang, J. Men, Q. Lei, Multi-functionality of cationic porphyrin-immobilized polymeric microspheres prepared by synchronously synthesizing and immobilizing pyridylporphyrin on surfaces of polymeric microspheres, *Mater. Chem. Phys.* 134 (2012) 1049-1058 doi:10.1016/j.matchemphys.2012.03.112
- [141] B. Gao, Y. Chen, Q. Lei, Realizing porphyrin-functionalization of crosslinked polystyrene microspheres via two special polymer reactions, *Polym. Adv. Technol.* 23 (2012) 491–499 doi: 10.1002/pat.1904
- [142] B. Gao, L. Fang, J. Men, Q. Lei, Synchronously synthesizing and immobilizing porphyrins on crosslinked polystyrene microspheres and preliminary study on catalytic activity of supported metalloporphyrins, *Polym. Adv. Technol.* 20 (2009) 1183–1189 doi: 10.1002/pat.1566

-
- [143] A.G. Griesbeck, A. Bartoschek, Sustainable photochemistry: solvent-free singlet oxygen-photooxygenation of organic substrates embedded in porphyrin-loaded polystyrene beads, *Chem. Commun.* 15 (2002) 1594 -1595 doi: 10.1039/B204017D
- [144] A.G. Griesbeck, T. T. El-Idreesy, Solvent-free photooxygenation of 5-methoxyoxazoles in polystyrene nanocontainers doped with tetrastyrilporphyrine and protoporphyrine IX, *Photochem. Photobiol. Sci.* 4 (2005) 205-209 doi: 10.1039/B416159A
- [145] J.J. Inbaraj, M.V. Vinodu, R. Gandhidasan, R. Murugesan, M. Padmarabhan, Photosensitising properties of ionic porphyrins immobilised on functionalised solid polystyrene support, *J. App. Polym. Sci.* 89 (2003) 3925-3930 doi: 10.1002/app12610
- [146] M.V. Vinodu, M. Padmanabhan, Electronic effect of polymeric environments on metalloporphyrins, *J. Polym. Sci. A. Polym. Chem.* 39 (2001) 326-334 doi: 10.1002/1099-0518(20010115)
- [147] Y. Wang, Y. Liu, G. Li, J. Hao, Porphyrin-based honeycomb films and their antibacterial activity, *Langmuir* 30 (2014) 6419-6426 doi: 10.1021/la501244s
- [148] M. Magaraggia, G. Jori, M. Sonari, C. L. Schofield, D. A. Russell, Porphyrin-silica microparticle conjugates as an efficient tool for the photosensitised disinfection of water contaminated by bacterial pathogens, *Photochem. Photobiol. Sci.* 12 (2013) 2170- 2176 doi: 10.1039/c3pp50282a
- [149] E. Alves, J.M.M. Rodrigues, M.A.F. Faustino, M.G.P.M.S. Neves, J.A.S. Cavaleiro, Z. Lin, A. Cunha, M.H. Nadais, J.P.C. Tome, A new insight on nanomagnet porphyrin hybrids for photodynamic inactivation of microorganisms, *Dyes Pigments* 110 (2014) 80-88 doi: 10.1016/j.dyepig.2014.05.016
- [150] C.M.B. Carvalho, E. Alves, L. Costa, J.P.C. Tome, M.A.F. Faustino, M.G.P.M.S. Neves, A.C. Tome, J.A.S. Cavaleiro, A. Almeida, A. Cunha, Z. Lin, J. Rocha, Functional cationic nanomagnet-porphyrin hybrids for the photoinactivation of microorganisms, *ACS Nano* 4 (2010) 7133-7140 doi: 10.1021/nn/026092
- [151] S.M. Ribeiro, A.C. Serra, A.M.d'A. Rocha Gonsalves, Covalently immobilized porphyrins on silica modified structures as photooxidation catalysts, *J. Mol. Catal. A: Chem.* 326 (2010) 121–127 doi: 10.1016/j.molcata.2010.05.001
- [152] R. Rychtarikova, S. Sabata, J. Hettflejs, G. Kuncova, Composites with photosensitive 5, 10, 15, 20-tetrakis (N-methylpyridinium-4-yl) porphyrin entrapped into silica gels, *J. Sol-Gel Sci. Techn.* 61 (2012) 119-125 doi: 10.1007/51097101/2600-y

-
- [153] J. Mosinger, O. Jirsák, P. Kubát, K. Lang B. Mosinger, Bactericidal nanofabrics based on photoproduction of singlet oxygen, *J. Mater. Chem.* 17 (2007) 164-166 doi: 10.1039/B614617a
- [154] M. Managa, E. Antunes, T. Nyokong, Conjugates of platinum nanoparticles with gallium tetra-(4-carboxyphenyl) porphyrin and their use in photodynamic antimicrobial chemotherapy when in solution or embedded in electrospun fiber, *Polyhedron* 76 (2014) 94-101 doi: 10.1016/j.pol.2014.03.050
- [155] P. Henke, H. Kozak, A. Artemenko, P. Kubát, J. Forstová, J. Mosinger, Superhydrophilic polystyrene nanofiber materials generating O₂ (¹Δ_g): postprocessing surface modifications toward efficient antibacterial effect, *ACS Appl. Mater. Interfaces*, 6 (2014) 13007-13014 doi: 10.1021/am502917w
- [156] Y. Lhotáková, L. Plíštil, A. Morávková, P. Kubát, K. Lang, J. Forstová, J. Mosinger, Virucidal nanofiber textiles based on photosensitized production of singlet oxygen, *PLoS One*, 7 (2011) e49226 doi: 10.1371/journal.pone.0049226
- [157] S. Jesenska, L. Plíštil, P. Kubat, K. Lang, L. Brozova, S. Popelka, L. Szatmary, J. Mosinger, Antibacterial nanofiber materials activated by light, *J. Biomed. Mater. Res. A* 99 (2011) 676–683 doi: 10.1002/jbm.a.33218
- [158] J. Sherrill, S. Michielsen, I. Stojiljkovic, Grafting of light-activated antimicrobial materials to nylon films, *J. Polym. Chem.* 41 (2003) 41-47 doi: 10.1002/pola.10556
- [159] J. Bozja, J. Sherrill, S. Michielsen, I. Stojiljkovic, Porphyrin-based, light activates antimicrobial materials, *J. Polym. Sci. A. Polym. Chem.* 41 (2003) 2297-2303 doi: 10.1002/pola.10773
- [160] A. K. Benabbou, C. Guillard, S. Pigeot-Remy, C. Cantau, T. Pigot, P. Lejeune, Z. Derriche, S. Lacombe, Water disinfection using photosensitizers supported on silica, *J. Photochem. Photobiol. A* 219 (2011) 101-108 doi:10.1016/j.jphotochem.2011.01.023
- [161] C. Cantau, S. Larribau, T. Pigot, M. Simon, M. T. Maurette, S. Lacombe, Oxidation of noxious sulfur compounds by photocatalysis or photosensitization, *Catal. Today* 122 (2007) 27–38 doi:10.1016/j.cattod.2007.01.038
- [162] C. Cantau, T. Pigot, N. Manoi, E. Oliveros, S. Lacombe, Singlet Oxygen in Microporous Silica Xerogel: Quantum Yield and Oxidation at the Gas–Solid Interface, *ChemPhysChem* 8 (2007) 2344–2353 doi: 10.1002/cphc.200700482
- [163] C.-P. Chen, C.-T., Chen T. Tsai, Chitosan nanoparticles for antimicrobial photodynamic inactivation: Characterization and in vitro investigation, *Photochem. Photobiol.* 88 (2011) 570-576 doi: 10.1111/j.1751-1097.2012.01101.x

-
- [164] M.Q. Mesquita, J.C.J.M.D.S. Menezes, S.M.G. Pires, M.G.P.M.S. Neves, M.M.Q. Simões, A.C. Tomé, J.A.S. Cavaleiro, A. Cunha, A.L. Daniel-da-Silva, A. Almeida, M.A.F. Faustino, Pyrrolidine-fused chlorin photosensitizer immobilized on solid supports for the photoinactivation of Gram negative bacteria, *Dyes Pigments* 110 (2014) 123–133 doi: 10.1016/j.dyepig.2014.04.025
- [165] M.Q. Mesquita, J.C.J.M.D.S. Menezes, M.G.P.M.S. Neves, A.C. Tomé, J.A.S. Cavaleiro, A. Cunha, A. Almeida, S. Hackbarth, B. Röder, M.A.F. Faustino, Photodynamic inactivation of bioluminescent *Escherichia coli* by neutral and cationic pyrrolidine-fused chlorins and isobacteriochlorins, *Bioorg. Med. Chem. Lett.* 24 (2014) 808–812 doi: 10.1016/j.bmcl.2013.12.097